DMD Fast Forward. Published on December 2, 2021 as DOI: 10.1124/dmd.121.000638
This article has not been copyedited and formatted. The final version may differ from this version.

Title Page

Title: Broad application of CYP3A4 LC-MS protein quantification in hepatocyte cytochrome P450 induction assays identifies nonuniformity in mRNA and protein induction responses[$]

Authors: John Paul Savaryn*, Jun Sun*, Junli Ma, Gary J. Jenkins, and David M. Stresser#

(*equal contribution; #corresponding author)

Author Affiliations: JPS, JS, JM, GJ, and DMS are affiliated with AbbVie Inc., DMPK-BA, North Chicago, IL

DMD Fast Forward. Published on December 2, 2021 as DOI: 10.1124/dmd.121.000638
This article has not been copyedited and formatted. The final version may differ from this version.

Running Title Page

Running Title: Broad profiling of the three CYP3A4 induction endpoints

Corresponding author name and contact information:

Name: David M. Stresser, Ph.D.

Address: 1 N Waukegan Rd. AP9, North Chicago, IL 60064, USA

Telephone number: 847-935-4327

Fax number: 847-938-9898

e-mail address: David.stresser@abbvie.com

Number of text pages: 25

Number of tables: 3

Number of figures: 4

Number of references: 35

Number of words in Abstract: 202

Number of words in Introduction: 588

Number of words in Discussion: 1505

List of abbreviations used: AhR, aryl hydrocarbon receptor; AUC, area under the curve; CAR, constitutive androstane receptor; CYP, cytochrome P450; DDI(s), drug-drug interaction(s); IQ, innovation and quality consortium; IWG, Induction Working Group; Ind, max, maximum induction; EC50, concentration that supports 50% of maximum response; Emax, maximum fold increase (or induction) minus baseline of 1-fold; Imax,u, maximal unbound concentrations in the plasma; PXR, pregnane-X receptor

DMD Fast Forward. Published on December 2, 2021 as DOI: 10.1124/dmd.121.000638
This article has not been copyedited and formatted. The final version may differ from this version.

Abstract

Screening for cytochrome P450 (CYP) induction potential is routine in drug development. Induction results in a net increase in CYP protein and is assessed typically by measuring indirect endpoints, *i.e.*, enzyme activity and mRNA in vitro. Recent methodological advancements have made CYP protein quantification by LC-MS in *in vitro* induction studies more accessible and amenable to routine testing. In this study, we evaluated CYP3A4 concentration dependence of induction response for 11 compounds (rifampin, rifabutin, carbamazepine, efavirenz, nitrendipine, flumazenil, pioglitazone, rosiglitazone, troglitazone, pazopanib, and ticagrelor) in plated hepatocytes from two or three donors incorporating in the assessment all three endpoints. In addition, the time-dependence of the induction was examined over 1, 2 or 3 days of treatment. For most compounds, mRNA, enzyme activity and protein endpoints exhibited similarity in induction responses. Pazopanib and ticagrelor were notable exceptions as neither protein nor enzyme activity were induced despite mRNA induction of a magnitude similar to efavirenz, pioglitazone or rosiglitazone, which clearly induced in all three endpoints. Static modeling of clinical induction responses supported a role for protein as a predictive endpoint. These data highlight the value of including CYP protein quantification as an induction assay endpoint to provide a more comprehensive assessment of induction liability.

DMD Fast Forward. Published on December 2, 2021 as DOI: 10.1124/dmd.121.000638
This article has not been copyedited and formatted. The final version may differ from this version.

Significance Statement

Direct, LC-MS-based quantification of CYP protein is a desirable induction assay endpoint, however the application of protein as an endpoint has been limited due to inefficient workflows. Here, we incorporate recent advancements in protein quantitation methods to efficiently quantify CYP3A4 protein in in vitro induction assays with 11 compounds in up to 3 donors. The data indicate induction responses from mRNA do not always align with those of protein suggesting assessment of induction liability is more complex than thought previously.

DMD Fast Forward. Published on December 2, 2021 as DOI: 10.1124/dmd.121.000638
This article has not been copyedited and formatted. The final version may differ from this version.

Introduction

A recent analysis of approximately 150 drugs approved by the USFDA between 2013 and 2017 indicated that 65% were substrates of CYP3A (Hakkola et al., 2020). Accordingly, in vitro evaluation of new drug candidates for CYP3A4 induction potential to elucidate drug-drug interaction potential is routinely conducted in drug discovery/development programs (EMA, 2012; FDA, 2020). Induction occurs as a result of an increase in rate of protein synthesis or decrease in rate of protein degradation (Hollenberg, 2002). For example, whereas rifampin causes de novo increase in rate of protein synthesis, erythromycin and troleandomycin may induce by decreasing the CYP3A protein degradation rate (Watkins et al., 1986). To evaluate CYP induction in vitro, quantifying relative changes in mRNA, and/or enzyme activity, is recommended (EMA, 2012; FDA, 2020). An assumption with mRNA analysis is that it is presumed to be a faithful proxy of induced protein whereas a drawback to measurements using enzyme activity is that it can be subject to inhibition by the test compound, potentially resulting in a masking of induction response (Hewitt et al., 2007). In principle, quantifying CYP protein changes directly would be preferable, but historical approaches (e.g. Western blotting) are considered only semi-quantitative and have been largely abandoned in the context of this assay.

In recent years, methods to quantify protein by LC-MS across broad applications has become commonplace. Adoption of LC-MS quantitation of protein in CYP induction studies has been hampered by inadequate analytical sensitivity, such that microsomal protein enrichment steps are required (Jenkins et al., 2006; Langenfeld et al., 2009; Kawakami et al., 2011; Sakamoto et al., 2011; Williamson et al., 2011; Xu et al., 2014). Recently, MacLean *et al.* applied immunoprecipitation to enrich CYP proteins to enable LC-MS protein quantification to complement the mRNA and activity endpoints in induction assays (MacLean et al., 2017). The value of quantifying protein was evident: in the example with the experimental compound BI-X, CYP3A4 mRNA was induced to a similar extent as it was with rifampin, however, the rise in CYP3A4 protein levels were only up to ~2-fold with BI-X compared to ~ 8 to 10-fold with rifampin across the three donors. Enzyme activity exhibited a similar, but more variable trend, to that

DMD Fast Forward. Published on December 2, 2021 as DOI: 10.1124/dmd.121.000638
This article has not been copyedited and formatted. The final version may differ from this version.

of protein. By monitoring all three endpoints, the authors suggested that mRNA alone was insufficient to fully evaluate induction potential of BI-X (MacLean et al., 2017). Despite the clear value of including protein quantitation as an endpoint, the efficiency of the immunoprecipitation step may not be sufficient to enable widespread adoption.

We recently developed an efficient, enrichment-free methodology for LC-MRM quantification of CYP3A4, CYP2B6, and CYP1A2 protein compatible with typical 96-well induction assay formats (Savaryn et al., 2020). Using this method, we sought to evaluate, on a wider scale, the CYP3A4 induction responses with all three endpoints with 11 different compounds using up to three hepatocyte donors. Compounds potentially expected to exhibit a variety of induction responses in vitro or in vivo were selected for our evaluation. To gain a full understanding of potential temporal differences in response among the endpoints, we also performed a time-course analysis of 24, 48, and 72 total hour incubation periods. Collectively, our data provide strong correlation in induction response among the three endpoints, but also identify empirical examples where CYP mRNA and protein induction relationship profiles differ markedly. These data suggest that addition of protein as an endpoint, coupled with mRNA and enzyme activity, may provide a more holistic assessment of in vivo induction response.

DMD Fast Forward. Published on December 2, 2021 as DOI: 10.1124/dmd.121.000638
This article has not been copyedited and formatted. The final version may differ from this version.

Materials and Methods

Test compounds and midazolam were obtained from MilliporeSigma (St. Louis, MO). 1'-Hydroxymidazolam-[$^{13}C_3$] was obtained from Corning Life Sciences.

Cell Culture and Drug Treatment

Cryopreserved primary human hepatocytes were purchased from BioIVT, USA. Briefly, hepatocytes were thawed and seeded directly onto collagen-coated 96-well culture plates (~55,000 cells/well) and overlaid with GelTrex™ extracellular matrix after 4-6 hours. Cells were cultured overnight, then treated with test compounds or vehicle control (0.1% DMSO) for 24-, 48- and 72 hours with daily change of treatment media; a 0 h time-point plate was also included, which were from hepatocytes plated and recovered overnight and without treatment. For concentration response testing, 6 to 8 concentrations were evaluated with concentrations chosen to achieve highest soluble concentrations and/or bracketing the total Cmax in human. A minimum of 5 concentrations was used to determine EC50 and Emax values; some values at high concentrations were excluded in curve fits due to apparent cytotoxicity.

RNA Isolation

The RNA was isolated using MagMAX™ Express 96 RNA Isolation System from ThermoFisher with RNA extraction kits (ThermoFisher, cat. no. AM1830). Hepatocytes were washed once with 1X PBS, followed by addition of 140 µL of RNA lysis buffer to each well and mixed to achieve lysis. The lysate was transferred to a well of the 96-well binding plate. The samples were then mixed with 20 µL magnetic bead solution according to the manufacturer's instruction. The beads with adhered RNA were captured on a 96-well magnetic tip manifold. The RNA sample beads were then washed and treated with TURBO™ DNase, followed by two buffer washes. The beads were then dried, and RNA was eluted with 50 µL elution buffer.

cDNA Synthesis and RT-PCR

DMD Fast Forward. Published on December 2, 2021 as DOI: 10.1124/dmd.121.000638
This article has not been copyedited and formatted. The final version may differ from this version.

cDNA synthesis was conducted following the protocol for SuperScript VILO™ Master Mix (ThermoFisher, cat. no. 11755250). Briefly, 4 µL of Master Mix were mixed with 16 µL of RNA followed by thermocycler incubation as follows: 25°C for 10 minutes; 42 °C for 60 minutes and terminated at 85°C for 5 minutes. RT-PCR was performed on ABI QuantStudio 7, with the following parameters: 2.5 µL of each cDNA sample was pipetted into a 96-well optical reaction plate (ThermoFisher/Applied Biosystems, cat. no. 4306737). Reagent mix was made using the TaqMan™ Fast Advanced Master Mix RT-PCR kit (ThermoFisher/Applied Biosystems, part no. 4444602). Seventeen and half microliters of each reagent mix was added to each well with 40 cycles of RT-PCR using TaqMan® Gene Expression Assay (ThermoFisher) with the following primer and probes:
Human CYP3A4, Cat. 4331182 Assay ID: Hs00604506_m1; GAPDH (control to account for any variability in RNA levels), Cat. 4351368 Assay ID: Hs02758991_g1.

CYP3A4 Enzyme Activity Assay

After one to three-day treatment with test compounds, the hepatocytes were washed with incubation medium, then incubated in 100 µL of medium containing 30 µM midazolam (Millipore Sigma) for 30 minutes. The CYP3A4 enzyme activity was quantified by LC-MS by measuring the formation of 1'-hydroxymidazolam using stable labeled internal standard C13-1'-hydroxymidazolam to control for signal fluctuation. For one of the five experiments, carbutamide was used as an internal standard with no apparent loss in data quality.

LC-MS/MS Protein Quantification

CYP3A4 protein was quantified using a surrogate peptide LC-MRM approach as described previously (Savaryn et al., 2020). In some cases, LC-MS run times were shortened to 1 minute per injection by using conventional HPLC at higher flow rates as follows: column = Kinetex 5µm, C18, 100 angstroms, 30 x 2.1 mm (Phenomenex), flow rate = 1500 uL/min, Mobile Phase A (MPA) = water + 0.1% formic acid, Mobile Phase B (MPB) = acetonitrile + 0.1% formic acid, gradient program = 0 – 0.2 min hold MPB at 3%, 0.2 – 0.75 min ramp MPB to 50%, 0.75 – 0.76 min ramp MPB to 95%, 0.76 – 0.86

DMD Fast Forward. Published on December 2, 2021 as DOI: 10.1124/dmd.121.000638
This article has not been copyedited and formatted. The final version may differ from this version.

min hold MPB at 95%, 0.86 – 0.87 min decrease MPB to 3%, 0.87 – 1.0 min hold MPB at 3%. This shortened run time using HPLC methodology is a significant improvement over our previous publication in terms of analytical throughput which used ~10 min per injection and UPLC conditions. Following in-plate processing and LC-MRM data acquisition, peak areas for three CYP3A4 surrogate tryptic peptides were determined using Skyline software (MacLean et al., 2010). Peak areas for each peptide were averaged across the replicate vehicle treated (0.1% DMSO) wells to serve as the denominator in calculating fold-change, to which peak areas from individual wells were normalized. The mean and standard deviation from triplicate samples were then calculated. Unless otherwise noted, the CYP3A4 protein data presented throughout this manuscript are from the LSLGGLLQPEKPVVLK peptide only, which we previously demonstrated as having the greatest magnitude of induction (Savaryn et al., 2020). Other surrogate peptides were examined in some cases and protein responses were similar, though slightly less sensitive (Supplemental Fig. 2). Quantification of basal CYP3A4 protein levels across an entire 96-well plate of untreated hepatocytes validated the ability of this method to detect even subtle changes in relative protein abundance, with an overall coefficient of variance of less than 15% across the plate (Supplemental Fig. 3).

Statistical analysis

Linear Regression: To verify the presence of induction responses, linear regression was performed with GraphPad PRISM® using the mean of triplicate measurements per concentration per donor as single Y-value entries in XY table format. Drug concentrations used in common across the three hepatocyte donors (ACB, VJX, QIE) and less than or equal to the Emax concentration (thereby analyzing initial slopes) in at least two of the three donors by mRNA were entered as X-values. Each replicate Y value (N=3, 1 mean value per donor X 3 donors) was considered as an individual point and auto settings were used for where to start and end the regression line. In the case of flumazenil, a negative control, data from two donors was used, but was otherwise as described above. Correlation analyses of mRNA, enzyme activity and

DMD Fast Forward. Published on December 2, 2021 as DOI: 10.1124/dmd.121.000638
This article has not been copyedited and formatted. The final version may differ from this version.

protein within and across each treatment period (e.g. 24, 48 and 72 h) was performed in PRISM using Pearson's correlation coefficient. A p value < 0.01 was deemed as statistically significant.

EC50/Ind,max curve fitting:

The EC50 and Ind,max values were generated by non-linear curve-fitting using a 4-parameter model, Y=Bottom + (X^Hillslope)*(Top-Bottom)/(X^HillSlope + EC50^HillSlope) with the bottom usually constrained to 1. Top values were constrained to the maximum response where indicated (see supplemental table 2). Unless initial fits exhibited Hill slopes < 2, the Hill Slope was constrained to < 2. We considered 1.7-fold induction coupled with evidence of concentration dependence as criteria to attempt curve fitting. Using 1.7-fold was an empirical choice in comparison to FDA-guidance of 2-fold, but we also sought to be more conservative in assigning presence or absence of induction response. Some values were excluded from curve fitting analysis, usually because they were > 20% lower than the maximum response and were at concentrations exceeding that giving the maximum response (e.g. exhibited a bell-shaped response).

R3 calculations

$$R3 = 1 / [1 + d \times ((Emax \times 10 \times Imax,u) / (EC50 + 10 \times Imax,u))]$$

R3 is the predicted ratio of intrinsic clearance values of a probe substrate for an enzymatic pathway in the absence and presence of an inducer. d is the scaling factor and was assumed to be 1. Emax is the maximum induction effect determined in vitro, equal to Ind, max fold-induction minus 1, or the span from the baseline to the maximum for sigmoidal fits not constrained to a baseline of 1. Imax,u is the maximal unbound plasma concentration of the interacting drug at steady state, which considering uncertainties in the protein binding measurements, the unbound fraction was set to 1% if experimentally determined to be <1% (see Supplemental Table 1 for actual parameters). EC50 is the concentration causing half-maximal effect determined in vitro.

DMD Fast Forward. Published on December 2, 2021 as DOI: 10.1124/dmd.121.000638
This article has not been copyedited and formatted. The final version may differ from this version.

Results

Concentration-response curves for CYP3A4 mRNA, enzyme activity and protein were generated for 11 compounds in hepatocytes from three donors (denoted ACB, VJX and QIE), with the exception that carbamazepine, efavirenz, nitrendipine and flumazenil were not evaluated in donor QIE. Rifampin (Fig. 1) served as a reference strong inducer, while flumazenil served as a non-inducing control. Among compounds exhibiting an induction response, mRNA was typically the most sensitive endpoint (Table 1). The three donors exhibited marked differences in the magnitude of mRNA fold induction; VJX exhibited maximum fold-induction that was 2- to 6-fold higher than in donors ACB and QIE, depending on the compound. Protein fold induction also varied across donors, but in contrast to the response with mRNA, donor VJX usually exhibited lowest fold induction of protein, in some cases undetectable when it was readily observed in the other two donors (e.g., rosiglitazone). The maximal induction response for enzyme activity, when present, was consistently greater than that for protein with donor VJX, similar with QIE, but consistently lower in donor ACB. Figure 2 depicts the marked inter-donor differences in magnitude and rank order of maximum fold induction for each of the three endpoints. In contrast to the variability in maximum fold induction, EC50 values were more similar across donors (Table 1).

Figure 3A-C shows the 48h concentration-response profile for pioglitazone, rosiglitazone and troglitazone, which have been well studied as potential inducers in vitro (Sahi et al., 2000; Sahi et al., 2003). With these compounds, mRNA, activity and protein induction responses broadly track together and all yield statistically significant increases in slope for each endpoint with concentration when aggregated across the 3 donors (Figure 3D). Rifampin, rifabutin, pioglitazone, carbamazepine, efavirenz and nitrendipine showed similar trends (Table 1). Flumazenil, a non-inducing control, did not show a statistically significant non-zero slope for any of the three endpoints when aggregated across the 2 donors tested (Supplemental Fig. 1). By contrast, pazopanib and ticagrelor exhibited induction of CYP3A4

DMD Fast Forward. Published on December 2, 2021 as DOI: 10.1124/dmd.121.000638
This article has not been copyedited and formatted. The final version may differ from this version.

mRNA only; enzyme activity and protein were not detectably induced (Fig. 4). After 48 h treatment, pazopanib induced mRNA in all three donors with max induction ranging from 5 – 15-fold (Fig. 4A). Enzyme activity was either unchanged, as in donor VJX, or reduced as in donors ACB and QIE (Fig. 4A). Protein was not induced in any of the three donors (Fig. 4A). Ticagrelor showed similar results as pazopanib for mRNA, albeit to a lesser degree (maximum induction 7-fold); activity was mostly unchanged with a slight decrease in activity in donor VJX, and protein was also unchanged (Fig. 4A). At 30 µM in donor ACB, ticagrelor exhibited a 3-4-fold induction in mRNA and activity, but was approximately 1-fold at 20 µM and not reproduced in a follow up time-course experiment with this donor or in other donors, suggesting this result was spurious (for a more detailed comparison of response within a compound across donors and endpoints, all 132 concentration-response figures generated in this study are shown in Supplemental Figure 1). Statistical analysis permitted a more objective comparison among the three endpoints for pazopanib and ticagrelor. This assessment showed that both compounds significantly induced mRNA, but not protein or activity (Fig. 4B). Pazopanib produced a statistically significant decrease in activity, as demonstrated by a negative slope (Fig. 4B) and this is consistent with its previously described role as a CYP3A4 time-dependent inhibitor (Mao et al., 2016). Use of 48 h incubation with 10 µM rifampin as an in-study positive control demonstrated sensitivity of the CYP3A4 protein induction endpoint in the pazopanib and ticagrelor studies across the three donors (Fig. 4C).

To further compare the temporal relationship of mRNA with activity and protein, we determined EC50 and Ind,max after 24, 48 and 72h exposures for rifampin, pazopanib, ticagrelor and rifabutin (Table 2, Supplemental Figure 1). In general, maximum fold-induction was observed at 72h regardless of endpoint, while EC50 values were generally unaffected by total exposure time. Despite the longer (and shorter) exposure times, pazopanib and ticagrelor again failed to exhibit meaningful induction responses for enzyme activity and protein (concentration dependence and ≥ 1.7-fold). Using this data set, we examined correlation coefficients across the 3 endpoints at each concentration (except concentrations exhibiting evidence of cytotoxicity). This analysis supported our conclusions with pazopanib and

DMD Fast Forward. Published on December 2, 2021 as DOI: 10.1124/dmd.121.000638
This article has not been copyedited and formatted. The final version may differ from this version.

ticagrelor showing no meaningful induction of activity or protein, although with some analyses statistically significant correlation ($p < 0.01$) was attained with mRNA vs protein and activity, despite fold induction well-below 1.7-fold for the latter endpoints (supplemental Fig. 4).

DMD Fast Forward. Published on December 2, 2021 as DOI: 10.1124/dmd.121.000638
This article has not been copyedited and formatted. The final version may differ from this version.

Discussion

Using a 'plate-to-peaks' LC-MS method for CYP protein quantification (Savaryn et al., 2020), we profiled CYP3A4 induction of protein as well as mRNA and enzyme activity for 11 compounds in three human hepatocyte donors. The efficiency of the method used here enabled a broad investigation of the relationship among the three induction endpoints, to our knowledge, for the first time. Whilst the use of mRNA as an endpoint has gained considerable popularity in the past 15 years (Fahmi et al., 2010; Zhang et al., 2014) and indeed is advocated by regulatory agencies, it is hampered by the need for assuming that mRNA translates in a predictable way into functional protein, and that this process is compound independent. Our findings suggest this is not always the case. As expected, induction responses differed between donors. One key finding was that the magnitude of response could differ greatly by endpoint. In a striking example, the most sensitive donor by mRNA was the least sensitive by protein (Table 1, Figure 2). Nevertheless, for most compounds in our test set, *directional* responses irrespective of magnitude, as well as EC50 values, among the three endpoints were largely similar (Table 1). However, ticagrelor and pazopanib were exceptions, with the 3 endpoints failing to correlate – mRNA was induced but not protein or enzyme activity. One explanation for these observations is that, unlike the more sensitive mRNA endpoint, induced protein and enzyme activity failed to meet a detection threshold. We believe this scenario to be unlikely, since the induction of mRNA by ticagrelor and pazopanib were of a similar or greater magnitude as efavirenz, pioglitazone or rosiglitazone in two or three donors (Table 1). The absence of protein or activity induction was not due to insufficient exposure time, since 72-hour exposures still failed to yield induced protein or activity. These data strongly suggest a post-transcriptional phenomenon, whereby P450 protein fails to be sufficiently translated or is degraded at a more rapid rate. Pazopanib exhibits CYP3A inactivation in HLM and plated hepatocytes (Mao et al., 2016). This may readily explain the absence of induction and the concentration-dependent decline in activity (Figure 4). However, one might expect induction of protein to be detectable, despite enzyme inactivation, as observed with ritonavir (Luo et al., 2002). On the other hand, adducted and/or damaged

DMD Fast Forward. Published on December 2, 2021 as DOI: 10.1124/dmd.121.000638
This article has not been copyedited and formatted. The final version may differ from this version.

CYP3A4 protein may be targeted for a faster degradation rate, as occurs after exposure to grapefruit constituents (Schmiedlin-Ren et al., 1997). Interestingly, Moscovitz *et al*. (2018) recently used RNA arrays to show the induction signature for pazopanib is distinct from PXR, CAR, or AhR pathways suggesting alternative pathways are operative (Moscovitz et al., 2018). Considering the present data, it is tempting to speculate that activation of such alternative pathways does not always lead to increased protein levels. With ticagrelor, an explanation for the absence of in vitro CYP3A4 protein or activity induction concurrently with induction of mRNA is less apparent. Zhou et al. observed no evidence of time-dependent inhibition of CYP3A4 but demonstrated activation and inhibition of midazolam 1'-hydroxylation and 4-hydroxylation (IC50 value, 8.2 μM), respectively (Zhou et al., 2011). Direct inhibition of midazolam catalysis by ticagrelor would not be anticipated in our catalytic activity assay as it should be sufficiently diluted by the media wash step prior to introduction of midazolam substrate. Unfortunately, we do not have an explanation why protein or activity was not induced despite relatively robust induction of mRNA.

Regulatory agencies provide a number of algorithms to assess induction responses in vivo from in vitro data (EMA, 2012; FDA, 2020). The R3 equation in the FDA guidance for *in vitro* DDI studies (FDA, 2020), incorporates EC50, Emax, and the observed or expected maximum unbound drug plasma concentration *in vivo* at steady state. We calculated R3 values for our test set using mRNA (per guidance) but also using activity and protein data inputs. For rifampin and thiazolidinedione compounds, all endpoints predicted reasonably well the correct direction and magnitude of AUC change in vivo of the CYP3A4 probe used (Table 3). However, for pazopanib the clinical data show an increase in CYP3A4 substrate AUC of 30%, in contrast to the 85% decrease in AUC predicted by R3. The observed data is consistent with the net effect of enzyme inhibition predominating over induction with pazopanib (Center for Drug Evaluation and Research, 2008; Goh et al., 2010). In this case, the *in vitro* induction assay with protein as the R3 endpoint would be more consistent with the observed data than the mRNA R3 prediction. For ticagrelor, the modest in vitro mRNA induction coupled with unbound exposure levels

DMD Fast Forward. Published on December 2, 2021 as DOI: 10.1124/dmd.121.000638
This article has not been copyedited and formatted. The final version may differ from this version.

indicated a 22% change in AUC, whereas no effect was indicated with activity and protein (Table 3). Although a 28% decrease in AUC was observed with midazolam, this outcome was attributed to a very unusual instance of in vivo activation of CYP3A4 by ticagrelor, rather than an induction response (Teng and Butler, 2013). Considering this mechanism, R3 calculations from all three in vitro endpoints were not contrary to the in vivo response. Despite some exceptions in this limited analysis, our data support the continued use of mRNA as a conservative, accessible and robust endpoint. However, concurrently our results suggest that acquiring all three endpoints has potential for a more informed assessment of the likely in vivo response and may eventually aid in supporting the deferral or elimination of unnecessary clinical drug-drug interaction studies.

As indicated earlier, the dynamic range of the protein quantification is lower than that of mRNA across donors and with one (e.g., VJX), dramatically so. This would place more scrutiny on the precision of the protein measurement to make inferences about the induction response. Indeed, the modest increases in CYP3A4 protein in donor VJX barely rises above 2-fold, the threshold often used to conclude induction of mRNA (EMA, 2012; FDA, 2020). Only in response to rifampin treatment did CYP3A4 protein rise above 2-fold induction for donor VJX. Fortunately, the precision of the method enables robust quantitation (e.g. <15% CV, Supp Fig. 3) which is evident upon inspection of fitted curves of triplicate data (Sup Fig. 1). Still, larger dynamic range would be desirable. Further, the observation that a large dynamic range in one endpoint for a given donor does not always equate with the others (e.g. VJX) poses challenges for donor qualification. If protein is to be included as an endpoint, the induction response as measured by fold-induction in protein should be evaluated prior to acquisition. All three of the donors in the current study were selected and acquired from the vendor primarily on the basis of post-thaw viability, morphology and mRNA-fold induction. However, with the present data set, we would conclude donor QIE emerges as a preferred donor for investigations requiring all three endpoints.

In principle, fold-induction of enzyme activity should not exceed that of protein. Therefore, it was interesting to observe enzyme activity Ind, max values exceed that of protein by ~ 2 to 5-fold (e.g., Table

DMD Fast Forward. Published on December 2, 2021 as DOI: 10.1124/dmd.121.000638
This article has not been copyedited and formatted. The final version may differ from this version.

1 and Figure 2) for donor VJX. This phenomenon also occurred with some compounds in donor QIE (up to 2.3-fold), but never with donor ACB. One explanation for the marked incongruity observed with donor VJX is that fold induction of CYP3A4 protein was underestimated. We do not believe this is the case because the same methodology and surrogate peptides were used with all donors, yet the observation was most peculiar to donor VJX. In addition, when we compared three different peptides selective for CYP3A4, we observed a similar protein induction response (see Supplemental Figure 2). Another potential explanation for our observations is that proteins potentially affecting P450 catalytic efficiency (e.g. NADPH cytochrome P450 reductase or cytochrome b5) or the pool of heme (e.g. aminolevulinic acid synthase 1) available for incorporation into holoenzyme, are induced to the extent that they augment catalytic activity in the induced state, but are rate-limiting for the basal, uninduced state (Maglich et al., 2002). Supplementation of exogenous cytochrome b5 was observed to attenuate substrate inhibition of 1'-hydroxylation of triazolam, a compound structurally similar to midazolam (Schrag and Wienkers, 2001). In the event midazolam was exhibiting substrate inhibition in hepatocytes, as has been shown in human liver microsomes (Podoll, 1996), induction of cytochrome b5 synthesis may stimulate midazolam activity without proportional induction of CYP3A4 protein. Disproportionate expression or induction of CYP3A5, another midazolam 1'-hydroxyase (Tseng et al., 2014), or P450-P450 isoform interactions affecting activity (Davydov and Prasad, 2021) also merit further investigation.

The recent and extensive body of work from the Innovation and Quality Consortium Induction Working Group (IQ IWG) (Kenny et al., 2018; Wong et al., 2020) has been impressive, providing recommendations on a number of questions pertaining to in vitro induction studies and drug-drug interaction risk-assessment. These investigations have focused on mRNA and enzyme activity as endpoints. With the wider adoption of protein quantitation methods including the present one, we anticipate a broader interrogation of the value of including protein measurements. The results with pazopanib, ticagrelor and BI-X (MacLean et al., 2017) suggest these investigations are warranted and may be useful in helping to augment induction risk assessment paradigms.

DMD Fast Forward. Published on December 2, 2021 as DOI: 10.1124/dmd.121.000638
This article has not been copyedited and formatted. The final version may differ from this version.

Acknowledgments

Authors would like to thank Hardikkumar Patel and Yueting Wang for bioanalytical support quantifying metabolite production in the CYP3A4 enzyme activity assays. Authors would also like to thank Xiazi Qiu for helpful discussion.

DMD Fast Forward. Published on December 2, 2021 as DOI: 10.1124/dmd.121.000638
This article has not been copyedited and formatted. The final version may differ from this version.

Authorship Contributions

Participated in research design: Savaryn, Sun, Jenkins, Stresser

*Conducted experiments**:*** Ma, Savaryn, Sun

Contributed new reagents or analytical tools: N/A

Performed data analysis: Ma, Sun, Savaryn, Stresser

Wrote or contributed to the writing of the manuscript: Savaryn, Sun, Stresser

DMD Fast Forward. Published on December 2, 2021 as DOI: 10.1124/dmd.121.000638
This article has not been copyedited and formatted. The final version may differ from this version.

References

Center for Drug Evaluation and Research (2008) Clinical Pharmacology and Biopharmaceutics Review(s). Available at https://www.accessdata.fda.gov/drugsatfda_docs/nda/2009/022465s000_ClinPharmR.pdf.

Davydov DR and Prasad B (2021) Assembling the P450 puzzle: on the sources of nonadditivity in drug metabolism. *Trends Pharmacol Sci*.

EMA (2012) Guideline on the investigation of drug interactions. . *Available at: https://wwwemaeuropaeu/en/documents/scientific-guideline/guideline-investigation-drug-interactions-revision-1_enpdf*.

Fahmi OA, Kish M, Boldt S, and Obach RS (2010) Cytochrome P450 3A4 mRNA is a more reliable marker than CYP3A4 activity for detecting pregnane X receptor-activated induction of drug-metabolizing enzymes. *Drug Metab Dispos* **38:**1605-1611.

Fahmi OA, Raucy JL, Ponce E, Hassanali S, and Lasker JM (2012) Utility of DPX2 cells for predicting CYP3A induction-mediated drug-drug interactions and associated structure-activity relationships. *Drug Metab Dispos* **40:**2204-2211.

FDA (2020) In Vitro Drug Interaction Studies - Cytochrome P450 Enzyme- and Transporter-Mediated Drug Interactions Guidance for Industry.

Goh BC, Reddy NJ, Dandamudi UB, Laubscher KH, Peckham T, Hodge JP, Suttle AB, Arumugham T, Xu Y, Xu CF, Lager J, Dar MM, and Lewis LD (2010) An evaluation of the drug interaction potential of pazopanib, an oral vascular endothelial growth factor receptor tyrosine kinase inhibitor, using a modified Cooperstown 5+1 cocktail in patients with advanced solid tumors. *Clin Pharmacol Ther* **88:**652-659.

Hakkola J, Hukkanen J, Turpeinen M, and Pelkonen O (2020) Inhibition and induction of CYP enzymes in humans: an update. *Arch Toxicol* **94:**3671-3722.

Hewitt NJ, Lecluyse EL, and Ferguson SS (2007) Induction of hepatic cytochrome P450 enzymes: methods, mechanisms, recommendations, and in vitro-in vivo correlations. *Xenobiotica* **37:**1196-1224.

Hollenberg PF (2002) Characteristics and common properties of inhibitors, inducers, and activators of CYP enzymes. *Drug Metab Rev* **34:**17-35.

Jenkins RE, Kitteringham NR, Hunter CL, Webb S, Hunt TJ, Elsby R, Watson RB, Williams D, Pennington SR, and Park BK (2006) Relative and absolute quantitative expression profiling of cytochromes P450 using isotope-coded affinity tags. *Proteomics* **6:**1934-1947.

Kawakami H, Ohtsuki S, Kamiie J, Suzuki T, Abe T, and Terasaki T (2011) Simultaneous absolute quantification of 11 cytochrome P450 isoforms in human liver microsomes by liquid chromatography tandem mass spectrometry with in silico target peptide selection. *J Pharm Sci* **100:**341-352.

Kenny JR, Ramsden D, Buckley DB, Dallas S, Fung C, Mohutsky M, Einolf HJ, Chen L, Dekeyser JG, Fitzgerald M, Goosen TC, Siu YA, Walsky RL, Zhang G, Tweedie D, and Hariparsad N (2018) Considerations from the Innovation and Quality Induction Working Group in Response to Drug-Drug Interaction Guidances from Regulatory Agencies: Focus on CYP3A4 mRNA In Vitro Response Thresholds, Variability, and Clinical Relevance. *Drug Metab Dispos* **46:**1285-1303.

Langenfeld E, Zanger UM, Jung K, Meyer HE, and Marcus K (2009) Mass spectrometry-based absolute quantification of microsomal cytochrome P450 2D6 in human liver. *Proteomics* **9:**2313-2323.

DMD Fast Forward. Published on December 2, 2021 as DOI: 10.1124/dmd.121.000638
This article has not been copyedited and formatted. The final version may differ from this version.

Luo G, Cunningham M, Kim S, Burn T, Lin J, Sinz M, Hamilton G, Rizzo C, Jolley S, Gilbert D, Downey A, Mudra D, Graham R, Carroll K, Xie J, Madan A, Parkinson A, Christ D, Selling B, LeCluyse E, and Gan LS (2002) CYP3A4 induction by drugs: correlation between a pregnane X receptor reporter gene assay and CYP3A4 expression in human hepatocytes. *Drug Metab Dispos* **30:**795-804.

MacLean B, Tomazela DM, Shulman N, Chambers M, Finney GL, Frewen B, Kern R, Tabb DL, Liebler DC, and MacCoss MJ (2010) Skyline: an open source document editor for creating and analyzing targeted proteomics experiments. *Bioinformatics* **26:**966-968.

MacLean C, Weiss F, Poetz O, and Ebner T (2017) Concept: The Use of Targeted Immunoaffinity Proteomics for Routine Assessment of In Vitro Enzyme Induction. *J Pharm Sci* **106:**3453-3457.

Maglich JM, Stoltz CM, Goodwin B, Hawkins-Brown D, Moore JT, and Kliewer SA (2002) Nuclear pregnane x receptor and constitutive androstane receptor regulate overlapping but distinct sets of genes involved in xenobiotic detoxification. *Mol Pharmacol* **62:**638-646.

Mao J, Tay S, Khojasteh CS, Chen Y, Hop CE, and Kenny JR (2016) Evaluation of Time Dependent Inhibition Assays for Marketed Oncology Drugs: Comparison of Human Hepatocytes and Liver Microsomes in the Presence and Absence of Human Plasma. *Pharm Res* **33:**1204-1219.

Moscovitz JE, Kalgutkar AS, Nulick K, Johnson N, Lin Z, Goosen TC, and Weng Y (2018) Establishing Transcriptional Signatures to Differentiate PXR-, CAR-, and AhR-Mediated Regulation of Drug Metabolism and Transport Genes in Cryopreserved Human Hepatocytes. *J Pharmacol Exp Ther* **365:**262-271.

Podoll TD (1996) Defining the Use of Midazolam as a Probe of CYP3A4 Activity: Sensitive Quantitation of the Metabolites and Characterization of Mechanism-Based Inactivation. *Doctoral Dissertation* **Available at: https://digital.lib.washington.edu/researchworks/bitstream/handle/1773/8160/9630102.pdf?sequence=1**

Sahi J, Black CB, Hamilton GA, Zheng X, Jolley S, Rose KA, Gilbert D, LeCluyse EL, and Sinz MW (2003) Comparative effects of thiazolidinediones on in vitro P450 enzyme induction and inhibition. *Drug Metab Dispos* **31:**439-446.

Sahi J, Hamilton G, Sinz M, Barros S, Huang SM, Lesko LJ, and LeCluyse EL (2000) Effect of troglitazone on cytochrome P450 enzymes in primary cultures of human and rat hepatocytes. *Xenobiotica* **30:**273-284.

Sakamoto A, Matsumaru T, Ishiguro N, Schaefer O, Ohtsuki S, Inoue T, Kawakami H, and Terasaki T (2011) Reliability and robustness of simultaneous absolute quantification of drug transporters, cytochrome P450 enzymes, and Udp-glucuronosyltransferases in human liver tissue by multiplexed MRM/selected reaction monitoring mode tandem mass spectrometry with nano-liquid chromatography. *J Pharm Sci* **100:**4037-4043.

Savaryn JP, Liu N, Sun J, Ma J, Stresser DM, and Jenkins G (2020) Enrichment-free High-throughput Liquid Chromatography-Multiple-Reaction Monitoring Quantification of Cytochrome P450 Proteins in Plated Human Hepatocytes Direct from 96-Well Plates Enables Routine Protein Induction Measurements. *Drug Metab Dispos* **48:**594-602.

Schmiedlin-Ren P, Edwards DJ, Fitzsimmons ME, He K, Lown KS, Woster PM, Rahman A, Thummel KE, Fisher JM, Hollenberg PF, and Watkins PB (1997) Mechanisms of enhanced oral availability of CYP3A4 substrates by grapefruit constituents. Decreased enterocyte CYP3A4 concentration and mechanism-based inactivation by furanocoumarins. *Drug Metab Dispos* **25:**1228-1233.

Schrag ML and Wienkers LC (2001) Triazolam substrate inhibition: evidence of competition for heme-bound reactive oxygen within the CYP3A4 active site. *Drug Metab Dispos* **29:**70-75.

Teng R and Butler K (2013) The effect of ticagrelor on the metabolism of midazolam in healthy volunteers. *Clin Ther* **35:**1025-1037.

Tseng E, Walsky RL, Luzietti RA, Jr., Harris JJ, Kosa RE, Goosen TC, Zientek MA, and Obach RS (2014) Relative contributions of cytochrome CYP3A4 versus CYP3A5 for CYP3A-cleared drugs assessed in vitro using a CYP3A4-selective inactivator (CYP3cide). *Drug Metab Dispos* **42:**1163-1173.

Watkins PB, Wrighton SA, Schuetz EG, Maurel P, and Guzelian PS (1986) Macrolide antibiotics inhibit the degradation of the glucocorticoid-responsive cytochrome P-450p in rat hepatocytes in vivo and in primary monolayer culture. *J Biol Chem* **261:**6264-6271.

Williamson BL, Purkayastha S, Hunter CL, Nuwaysir L, Hill J, Easterwood L, and Hill J (2011) Quantitative protein determination for CYP induction via LC-MS/MS. *Proteomics* **11:**33-41.

Wong SG, Ramsden D, Dallas S, Fung C, Einolf HJ, Palamanda J, Chen L, Goosen TC, Siu YFA, Zhang G, Tweedie DJ, Hariparsad N, Jones BC, and Yates PD (2020) Considerations from the Innovation and Quality Induction Working Group in Response to Drug-Drug Interaction Guidance from Regulatory Agencies: Guidelines on Model Fitting and Recommendations on Time Course for In Vitro CYP Induction Studies Including Impact on Drug Interaction Risk Assessment. *Drug Metab Dispos*.

Xu L, Ma B, Yu S, Xia C, and Wu JT (2014) The use of a rapid MS-based method for the quantification of the CYP 3A4 protein directly from hepatocyte cell lysate for CYP induction studies. *Bioanalysis* **6:**3271-3282.

Zhang JG, Ho T, Callendrello AL, Clark RJ, Santone EA, Kinsman S, Xiao D, Fox LG, Einolf HJ, and Stresser DM (2014) Evaluation of calibration curve-based approaches to predict clinical inducers and noninducers of CYP3A4 with plated human hepatocytes. *Drug Metab Dispos* **42:**1379-1391.

Zhou D, Andersson TB, and Grimm SW (2011) In vitro evaluation of potential drug-drug interactions with ticagrelor: cytochrome P450 reaction phenotyping, inhibition, induction, and differential kinetics. *Drug Metab Dispos* **39:**703-710.

Footnotes

[$] **Disclosure:** All authors are or were employees of AbbVie at the time the work was conducted and may own AbbVie stock. AbbVie sponsored and funded the study; contributed to the design; participated in the collection, analysis, and interpretation of data, and in writing, reviewing, and approval of the final publication.

DMD Fast Forward. Published on December 2, 2021 as DOI: 10.1124/dmd.121.000638
This article has not been copyedited and formatted. The final version may differ from this version.

Figure Legends

Figure 1. Donor-to-donor variability in CYP3A4 induction profiles by rifampin. Human hepatocytes from three donors were cultured in 96-well plates and treated for 48 h (2 X 24h treatments) with increasing concentrations of rifampin. CYP3A4 induction was assessed using activity (red), mRNA (blue), and protein (black) endpoint assays. For each endpoint, data are presented as fold induction compared to vehicle treated control. Data are the mean and standard deviation of triplicate wells. Levels in vehicle control wells (one-fold) and 1.7-fold induction are indicated by dashed lines. Activity data were excluded for Donor ACB at 30 µM due to aberrant LC-MS/MS internal standard behavior.

Figure 2. Induction max (or when fit was not possible for ticagrelor mRNA and activity, indicated by square symbols, maximum fold-induction) for the 11 compounds tested across the donors shown, for each endpoint. Data are from Table 1. Connector lines indicate responses with same compound. Absence of connector lines indicate any induction response was below 1.7-fold threshold value. Note: donor QIE did not have data for carbamazepine, efavirenz, nitrendipine or flumazenil and therefore fewer data points are available for this donor.

Figure 3. Effect of thiazolidinedione family compounds on CYP3A4 induction determined by enzyme activity, mRNA or protein. Human hepatocytes from three donors were cultured in 96-well plates and treated for 48 h (2 X 24h treatments) with increasing concentrations of pioglitazone, rosiglitazone, or troglitazone. CYP3A4 induction was assessed using activity (red), mRNA (blue), and protein (black) endpoint assays. A) Donor ACB; B) Donor VJX; C) Donor QIE. For each endpoint, data are presented as fold induction compared to vehicle treated control. Data are the mean and standard deviation of triplicate wells. Levels in vehicle control wells (one-fold) and 1.7-fold induction are indicated by dashed lines. D) Linear regression of the data from all three donors (A-C). For regression analysis, triplicate means per concentration per donor were treated as single values. Thus, regression was performed with N=3 per concentration, one value per concentration per donor X 3 donors. The datapoints

DMD Fast Forward. Published on December 2, 2021 as DOI: 10.1124/dmd.121.000638
This article has not been copyedited and formatted. The final version may differ from this version.

in (D) represent the mean of the N=3 values per concentration. The dashed line represents baseline (one-fold) CYP3A4 levels in vehicle control. The 30 µM troglitazone data were omitted for linear regression due to saturation of response.

Figure 4. Effect of pazopanib and ticagrelor on CYP3A4 induction determined by enzyme activity, mRNA or protein. A) Human hepatocytes from three donors were cultured in 96-well plates and treated for 48 h (2 X 24 h treatments) with increasing concentrations of pazopanib (top) or ticagrelor (bottom). CYP3A4 induction was assessed using activity (red), mRNA (blue), and protein (black) endpoint assays. Data are the mean and standard deviation of triplicate wells, except for the activity data in the 30 µM ticagrelor treatment in Donor ACB, which is N = 2 wells due to an analytical error. Levels in vehicle control wells (one-fold) and 1.7-fold induction are indicated by dashed lines. B) Linear regression of the data from all three donors in A above. For regression analysis, triplicate means per concentration per donor were treated as single values. Thus, regression was performed with N=3 per concentration, one value per concentration per donor X 3 donors. The datapoints in B represent the mean of the N=3 values per concentration. C) CYP3A4 protein levels after 48 h (2 x 24 h treatments) incubation with 10 µM rifampin across the three donors and same studies as in A & B above. Data are the mean and standard deviation of 6 replicate wells for vehicle (0.1% DMSO) and triplicate wells for rifampin treatment. Levels in vehicle control wells (one-fold) and 1.7-fold induction are indicated by dashed lines.

Tables

Table 1. EC50 and Ind,max values, 48 h single time-point assays in plated human hepatocyte donor ACB, VJX and QIE

		ACB			VJX			QIE		
Drugs		mRNA	Activity	Protein	mRNA	Activity	Protein	mRNA	Activity	Protein
Rifampin	EC50 (μM)	0.19, 0.17, 0.19	0.26, 0.37, 0.14	0.30, 0.41, 0.38	0.91, 0.43	0.41, 0.70	0.84, 0.36	0.17, 0.31	0.15, 0.13	0.38, 0.26
Rifabutin	EC50 (μM)	0.96, 0.96	-[a], 0.18	-[b], 0.2	2.0	0.12	0.24	0.32	0.14	0.2
Pazopanib	EC50 (μM)	3.7, 4.7	-	-	3.9	-	-	3.6	-	-
Ticagrelor	EC50 (μM)	-[c], 4.2	-[c], -	-	6.5	-	-	5.5	-	-
Pioglitazone	EC50 (μM)	-	-	-	5.0	4.4	-	13	12	13
Rosiglitazone	EC50 (μM)	15	11	12	13	14	-	15	11	15
Troglitazone	EC50 (μM)	6.8	3.5	4.2	5.9	4.3	2.4	3.9	1.0	1.8
Carbamazepine	EC50 (μM)	18	12	22	59	29	28	ND	ND	ND
Efavirenz[d]	EC50 (μM)	2.3	2.3	3.9	3.3	3.5	-	ND	ND	ND
Nitrendipine	EC50 (μM)	11	1.2	3.1	12	3.4	-	ND	ND	ND
Flumazenil	EC50 (μM)	-	-	-	-	-	-	ND	ND	ND
Rifampin	Ind_{max} (fold)	13, 11, 18	3.0, 2.6, 2.4	8.1, 4.1, 6.9	63, 34	5.4, 12	2.8, 2.3	14, 25	8.3, 9.9	12, 11
Rifabutin	Ind_{max} (fold)	18, 13	-[a], 2.1	-[b], 2.9	116	3.6	1.6	31	6.6	2.9
Pazopanib	Ind_{max} (fold)	5.8, 5.3	-	-	16	-	-	7.3	-	-
Ticagrelor	Ind_{max} (fold)	3.2[e], 2.2	3.9[e], -	-	6.7	-	-	3.5	-	-
Pioglitazone	Ind_{max} (fold)	-	-	-	6.6	3.4	-	7.3	4.6	3.6
Rosiglitazone	Ind_{max} (fold)	3.8	2.4	3.3	20	7.6	-	5.9	8.4	5.9
Troglitazone	Ind_{max} (fold)	12	2.5	4.8	25	6.4	1.9	23	6.2	4.3
Carbamazepine	Ind_{max} (fold)	9.9	2.3	5.2	58	3.6	1.7	ND	ND	ND
Efavirenz[d]	Ind_{max} (fold)	5.6	2.6	4.4	21	7.3	-	ND	ND	ND
Nitrendipine	Ind_{max} (fold)	9.3	1.7	4.0	40	3.6	-	ND	ND	ND

Flumazenil	Ind_{max} (fold)	-	-	-	-	-	-	ND	ND	ND

Dashes (-) indicate no induction response (e.g. < 1.7-fold or a span of 0.7); ND, Not done

[a] *– No fit; 2.8-fold induction observed at 0.3 µM then > 20% concentration-dependent decline at 1 µM and higher*

[b] *– No fit; 4 values ranging from 2.4-fold and 3.5-fold at concentrations 0.1 (lowest concentration in experiment), 0.3, 1 and 3 µM.*

[c] *– No curve was fit because no concentration-response was observed.*

[d] *– Top two concentrations (20 and 30 µM) excluded from fits for both donors because of significant and concentration dependent down-turn in response*

[e] *– No curve was fit because no concentration-response was observed. Maximum fold-induction is shown at 30 µM*

Table 2. EC_{50} and Ind_{max} values, time-course assays from plated human hepatocytes in donor ACB

Drugs	Time Points (hr)	EC_{50} (μM)			Ind_{max} (Fold)		
		mRNA	Activity	Protein	mRNA	Activity	Protein
Rifampin	24	0.25	-[a]	0.27	9.9	-	2.2
	48	0.17	0.37	0.41	11	2.6	4.1
	72	0.29	0.26	0.52	20	3.8	7.4
Pazopanib	24	3.6	-	-	3.2	-	-
	48	4.7	-	-	5.3	-	-
	72	3.6	-	-	5.4	-	-
Ticagrelor	24	7.6	-	-	2.3	-	-
	48	4.2	-	-	2.2	-	-
	72	3.9	-	-	2.7	-	-
Rifabutin	24	0.61	-	0.13	11	-	1.8
	48	0.96	0.18	0.20	13	2.1	2.9
	72	0.95	0.18	0.22	18	3.9	3.9

[a] – *Dashes ("-") indicate insufficient induction responses for EC_{50} or Ind_{max} determination (< 1.7-fold)*

Table 3. R3 predictions versus observed clinical data

	R3												CYP3A4 substrate *in vivo* AUC				References for Observed *in vivo* data
	mRNA			Activity			Protein			Average (SD[a])			Predicted				
Drug	ACB	VJX	QIE	ACB	VJX	QIE	ACB	VJX	QIE	mRNA	Activity	Protein	mRNA	Activity	Protein	Observed	
Rifampin	0.07	0.02	0.05	0.40	0.12	0.11	0.16	0.39	0.09	0.05 (0.03)	0.21 (0.17)	0.21 (0.16)	↓95%	↓79%	↓79%	↓97%[c]	(Fahmi et al., 2012)
Pazopanib	0.22	0.08	0.16	ND[b]	ND[b]	ND[b]	ND[b]	ND[b]	ND[b]	0.15 (0.07)	ND[b]	ND[b]	↓85%	ND[b]	ND[b]	↑30%[c]	(Goh et al., 2010)
Ticagrelor	0.85	0.64	0.85	ND[b]	ND[b]	ND[b]	ND[b]	ND[b]	ND[b]	0.78 (0.12)	ND[b]	ND[b]	↓22%	ND[b]	ND[b]	↓30%[c]	(Teng and Butler, 2013)
Pioglitazone	ND[b]	0.77	0.88	0.99	0.88	0.93	0.94	0.96	0.95	0.83 (0.08)	0.93 (0.06)	0.95 (0.01)	↓17%	↓7%	↓5%	↓26%[c]	(Fahmi et al., 2012)
Rosiglitazone	0.98	0.83	0.93	0.98	0.94	0.92	0.97	ND[b]	0.96	0.91 (0.07)	0.94 (0.03)	0.97 (0.01)	↓9%	↓6%	↓3%	↓12%[d]	(Fahmi et al., 2012)
Troglitazone	0.51	0.30	0.25	0.81	0.59	0.33	0.67	0.85	0.54	0.35 (0.14)	0.58 (0.24)	0.69 (0.15)	↓65%	↓42%	↓31%	↓67%[c]	(Fahmi et al., 2012)
Rifabutin	0.12	0.02	0.06	0.52	0.30	0.17	0.39	0.62	0.21	0.07 (0.05)	0.33 (0.18)	0.41 (0.21)	↓93%	↓67%	↓59%	↓35%[e]	(Fahmi et al., 2012)
Carbamazepine	0.13	0.03	ND[b]	0.47	0.35	ND[b]	0.25	0.62	ND[b]	0.08 (0.07)	0.41 (0.09)	0.44 (0.27)	↓92%	↓59%	↓56%	↓94%[c]	(Fahmi et al., 2012)
Efavirenz	0.47	0.21	ND[b]	0.71	0.47	ND[b]	0.64	0.89	ND[b]	0.34 (0.18)	0.59 (0.17)	0.77 (0.17)	↓66%	↓41%	↓23%	↓41%[f]	(Fahmi et al., 2012)
Nitrendipine	0.99	0.98	ND[b]	0.99	0.99	ND[b]	0.99	1.00	ND[b]	0.98 (0.01)	0.99 (0.001)	0.99 (0.003)	↓2%	↓1%	↓1%	↑10%[c]	(Fahmi et al., 2012)

[a] - SD = Standard Deviation, [b] - ND = Not Determined, Victim Drug = [c] - midazolam, [d] - nifedipine, [e] - EE, [f] - atorvastatin

DMD Fast Forward. Published on December 2, 2021 as DOI: 10.1124/dmd.121.000638
This article has not been copyedited and formatted. The final version may differ from this version.

DMD Fast Forward. Published on December 2, 2021 as DOI: 10.1124/dmd.121.000638
This article has not been copyedited and formatted. The final version may differ from this version.

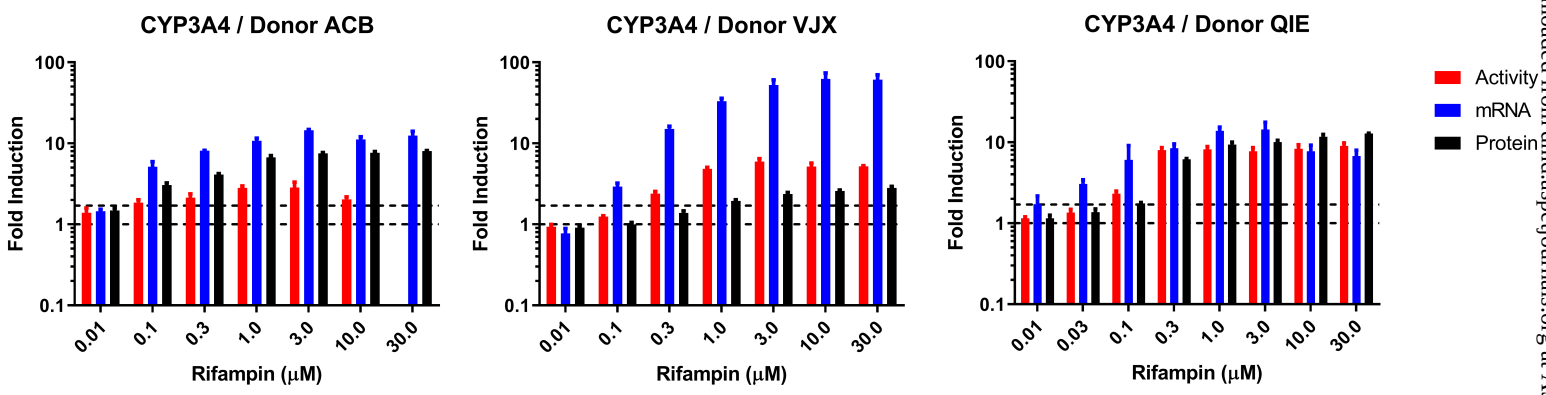

Figure 1

DMD Fast Forward. Published on December 2, 2021 as DOI: 10.1124/dmd.121.000638
This article has not been copyedited and formatted. The final version may differ from this version.

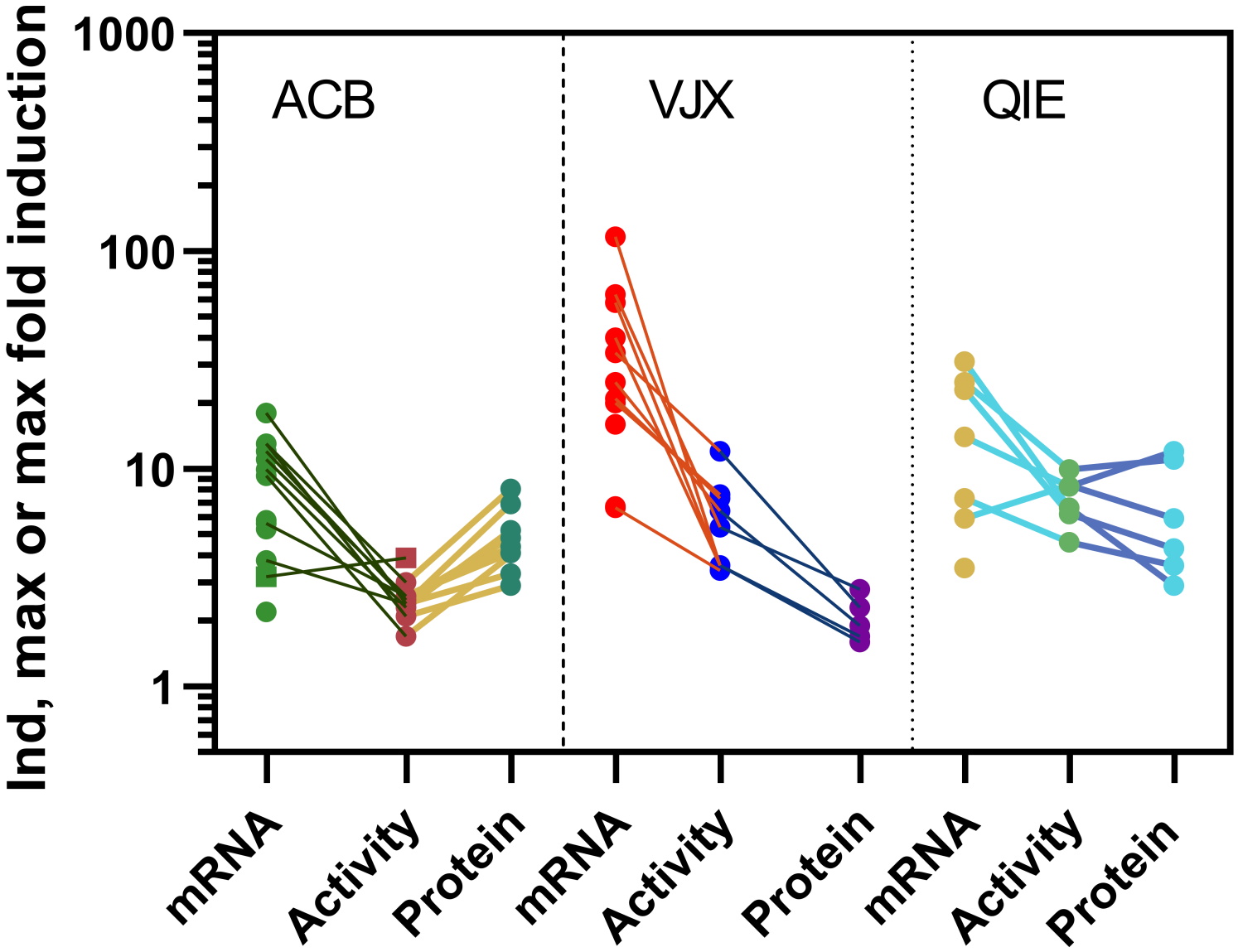

Figure 2

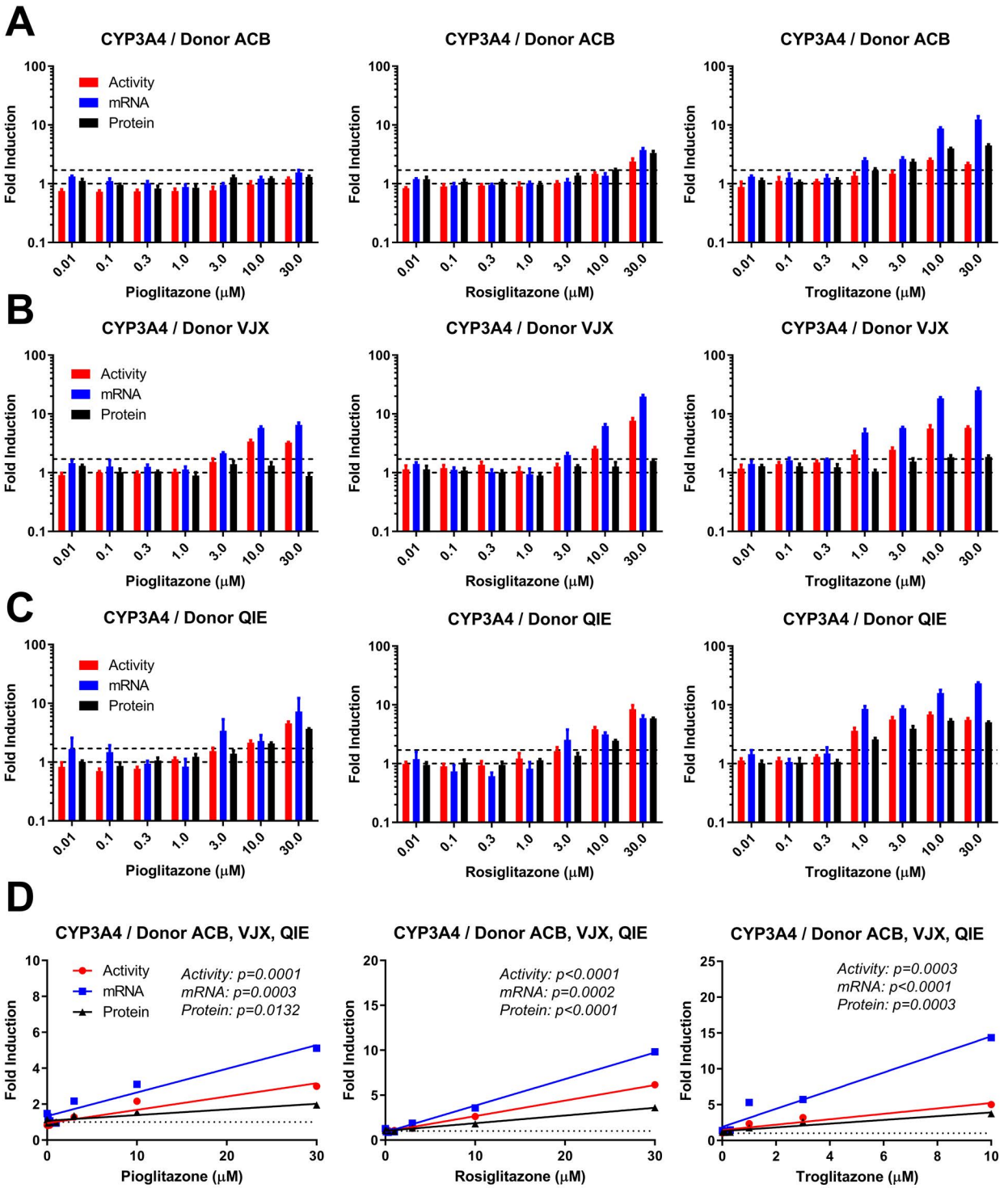
A
CYP3A4 / Donor ACB
CYP3A4 / Donor ACB
CYP3A4 / Donor ACB
Activity
mRNA
Protein
Fold Induction
100
10
1
0.1
0.01
0.1
0.3
1.0
3.0
10.0
30.0
Pioglitazone (μM)
Rosiglitazone (μM)
Troglitazone (μM)
B
CYP3A4 / Donor VJX
CYP3A4 / Donor VJX
CYP3A4 / Donor VJX
C
CYP3A4 / Donor QIE
CYP3A4 / Donor QIE
CYP3A4 / Donor QIE
D
CYP3A4 / Donor ACB, VJX, QIE
CYP3A4 / Donor ACB, VJX, QIE
CYP3A4 / Donor ACB, VJX, QIE
Activity: p=0.0001
mRNA: p=0.0003
Protein: p=0.0132
Activity: p<0.0001
mRNA: p=0.0002
Protein: p<0.0001
Activity: p=0.0003
mRNA: p<0.0001
Protein: p=0.0003

Figure 3

DMD Fast Forward. Published on December 2, 2021 as DOI: 10.1124/dmd.121.000638
This article has not been copyedited and formatted. The final version may differ from this version.

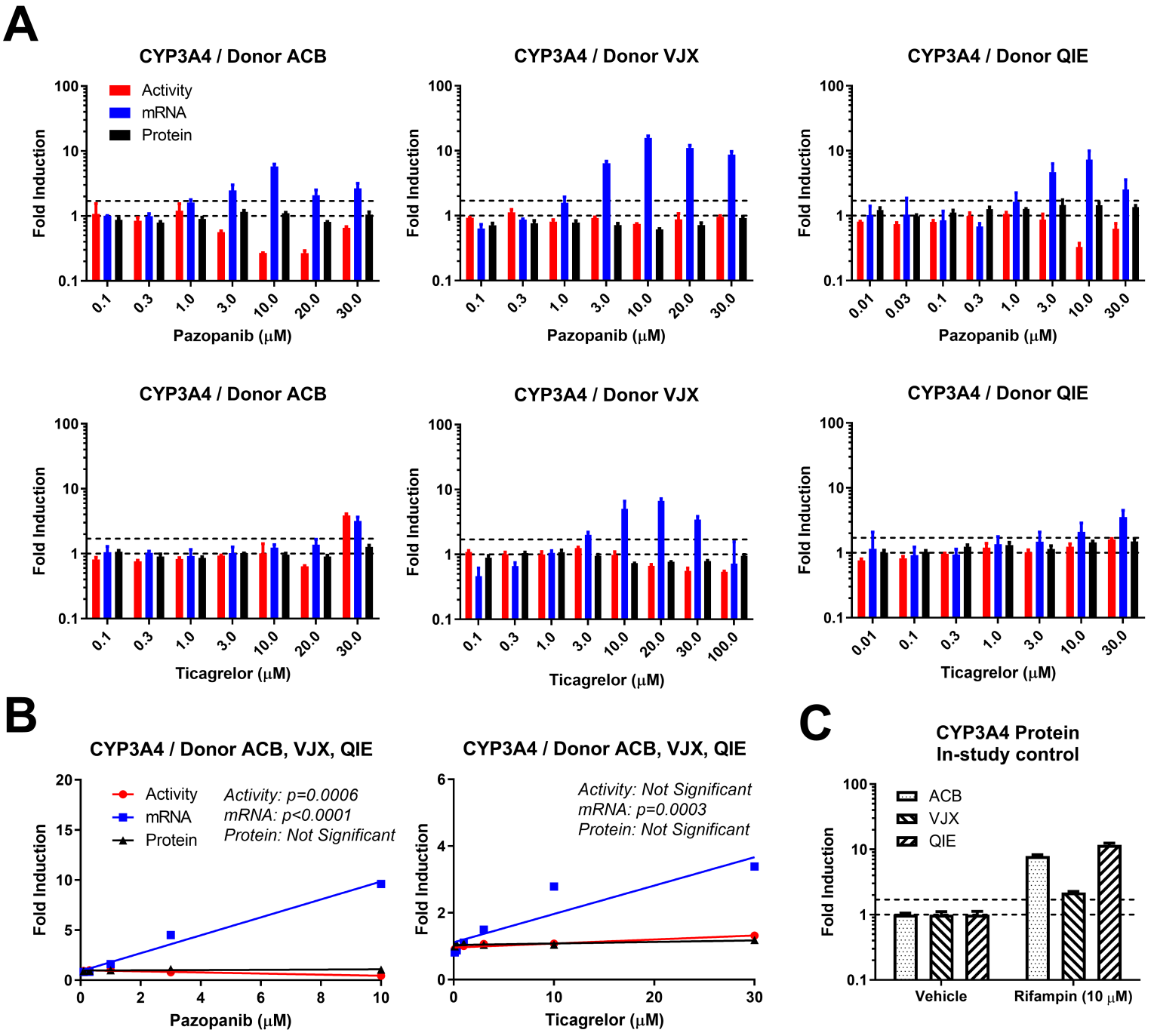

Figure 4

Supplemental Material

Article Title: Broad application of CYP3A4 LC-MS protein quantification in hepatocyte cytochrome P450 induction assays identifies nonuniformity in mRNA and protein induction responses

Authors: John Paul Savaryn*, Jun Sun*, Junli Ma, Gary Jenkins, and David M. Stresser#

(*equal contribution; #corresponding author)

Journal Title: Drug Metabolism and Disposition

Manuscript number: DMD-AR-2021-000638

Supplemental Figure 1. Concentration-response curves for the 132 compound/donor hepatocyte experiments in this study.

Rifampin	mRNA	Activity	Protein
ACB (1)	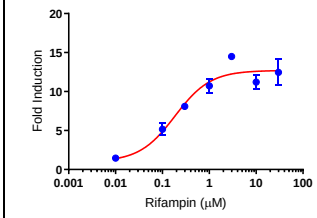	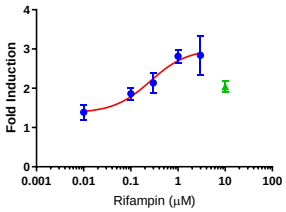	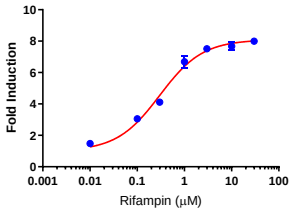
VJX (2)	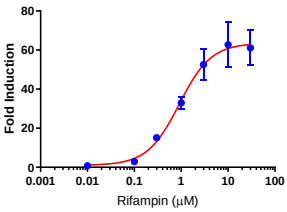	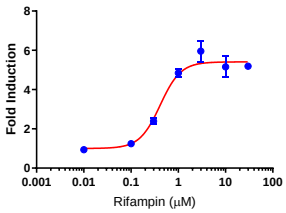	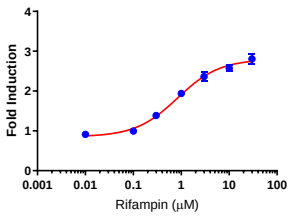
QIE (3) – plate 1	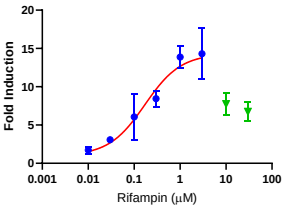	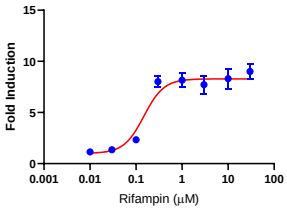	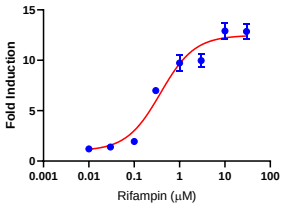
QIE (3) – plate 2	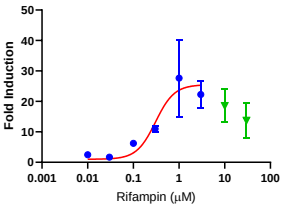	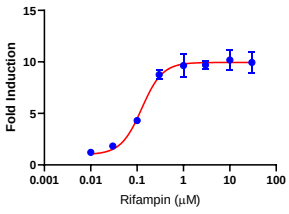	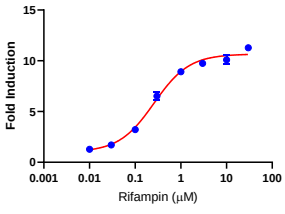
ACB (4) - 24h	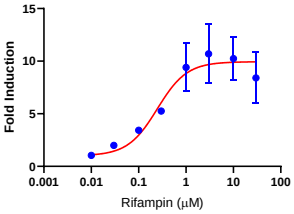	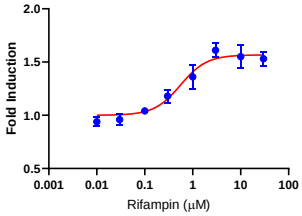	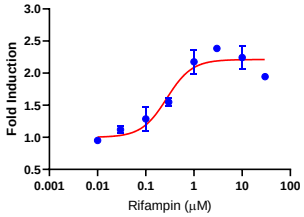
ACB (4) - 48h	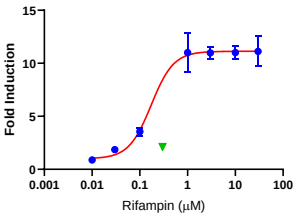	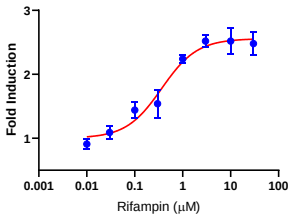	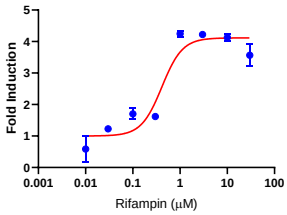

ACB (4) - 72h	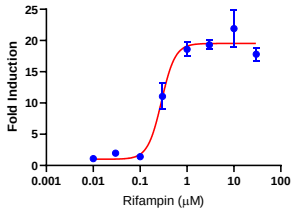	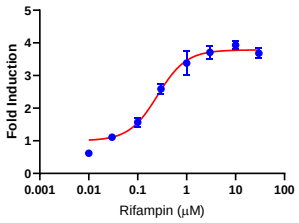	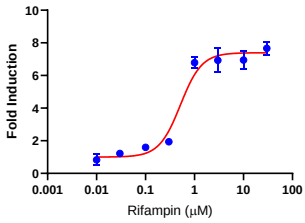
ACB (5)	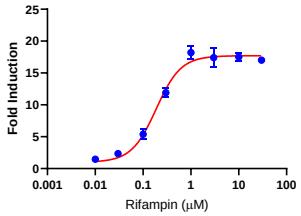	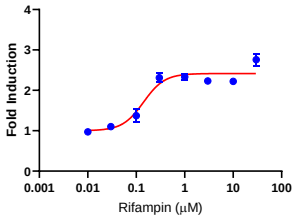	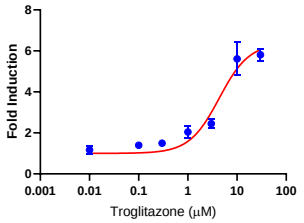
VJX (5)	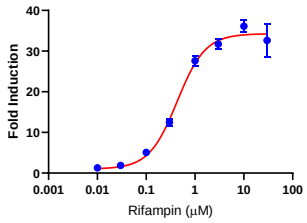	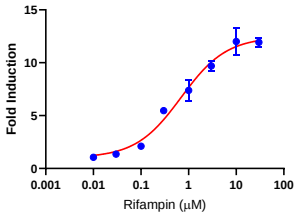	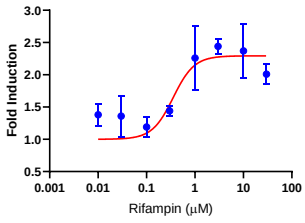

Rifabutin	mRNA	Activity	Protein
ACB (1)	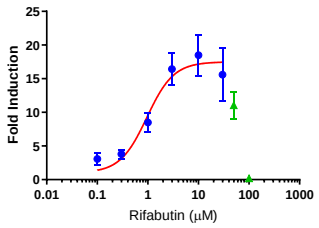	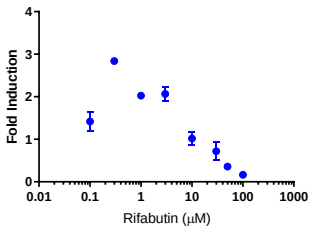	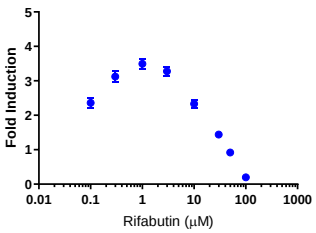
VJX (2)	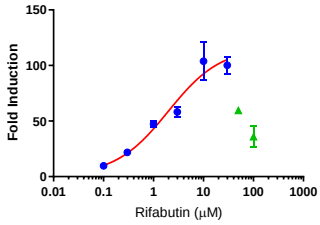	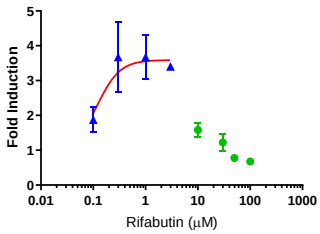	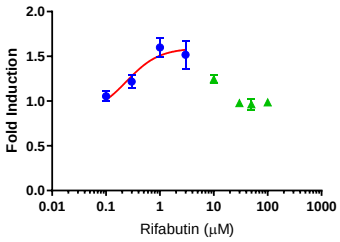
QIE (3)	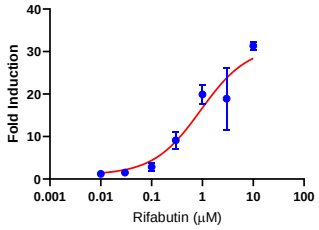	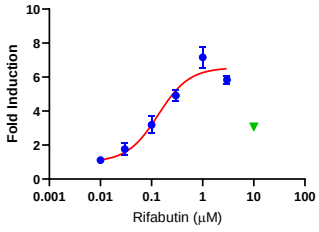	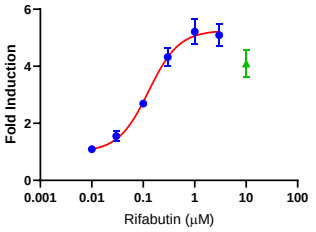
ACB (4) - 24h	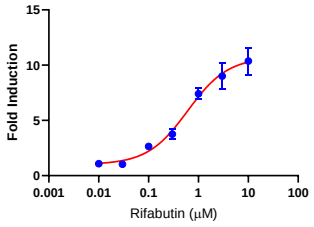	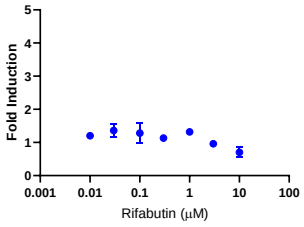	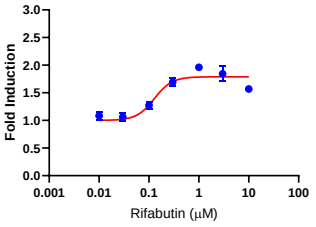
ACB (4) - 48h	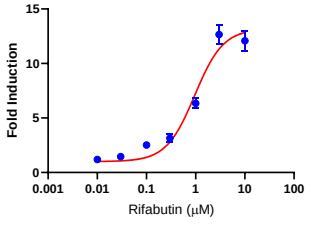	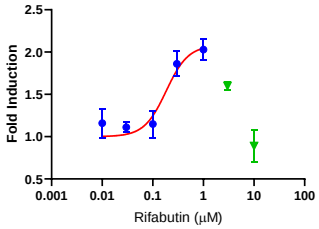	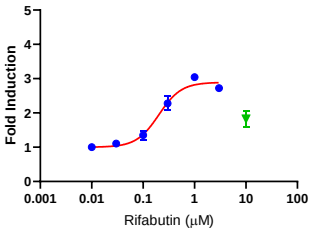
ACB (4) - 72h	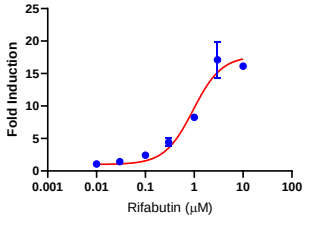	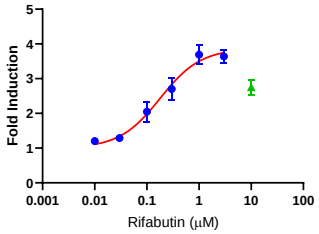	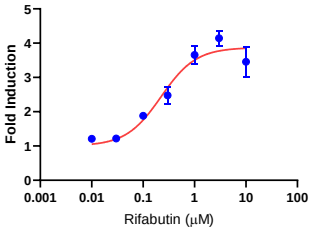

Pazopanib	mRNA	Activity	Protein
ACB (1)	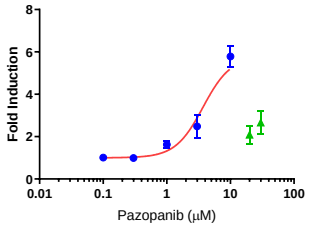	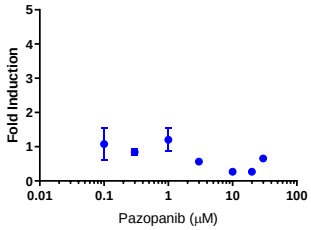	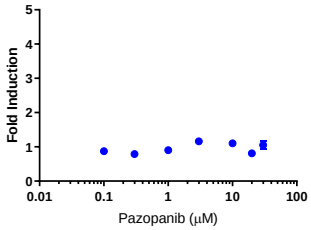
VJX (2)	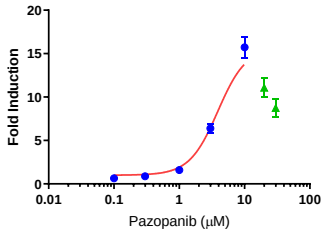	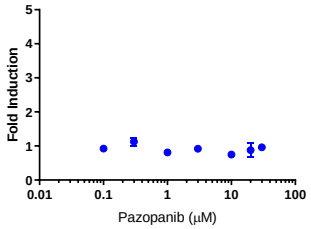	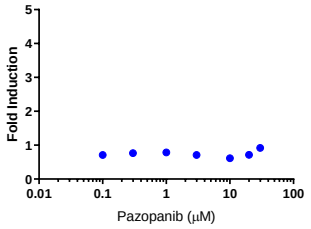
QIE (3)	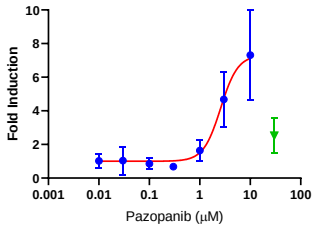	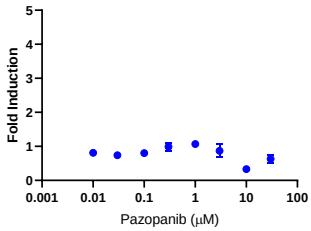	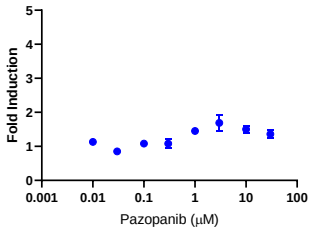
ACB (4) - 24h	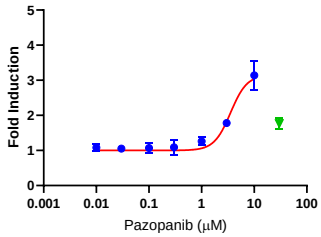	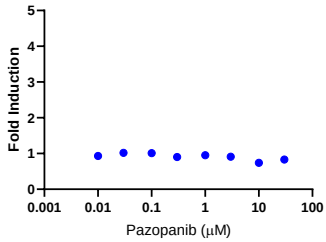	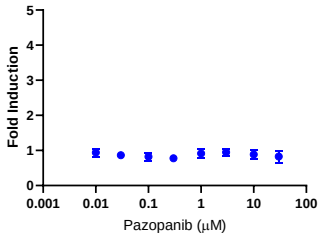
ACB (4) - 48h	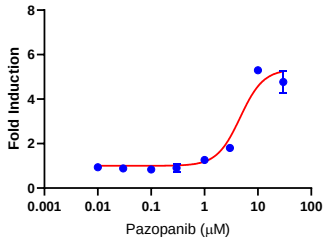	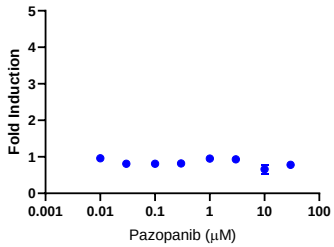	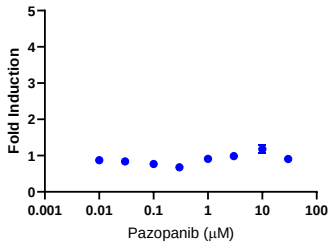
ACB (4) - 72h	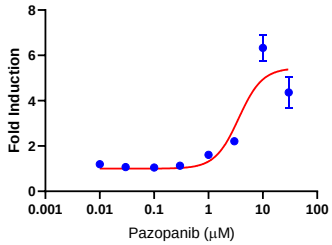	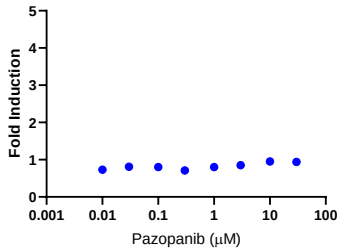	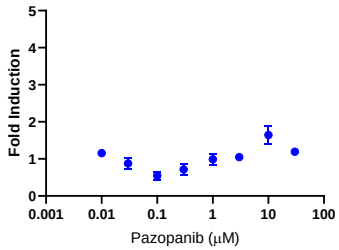

Ticagrelor	mRNA	Activity	Protein
ACB (1)	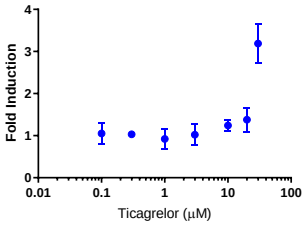	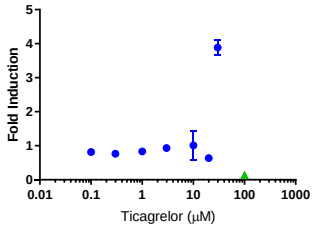	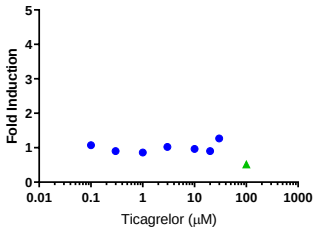
VJX (2)	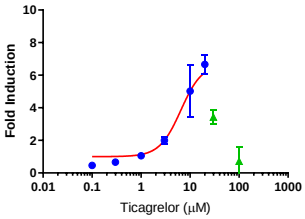	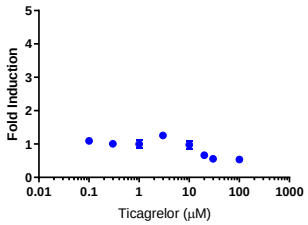	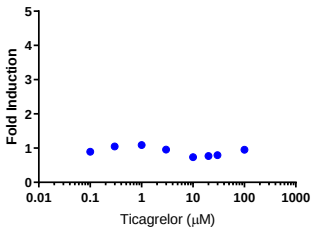
QIE (3)	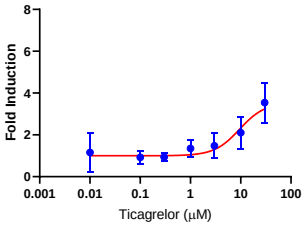	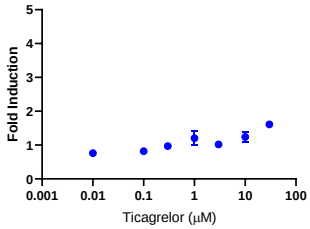	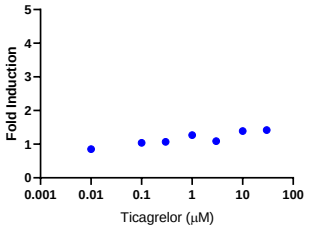
ACB (4) - 24h	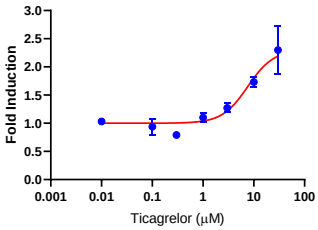	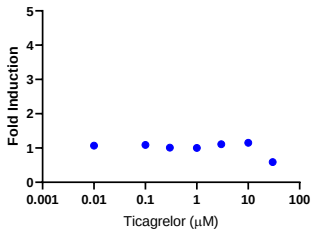	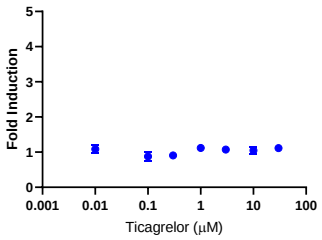
ACB (4) - 48h	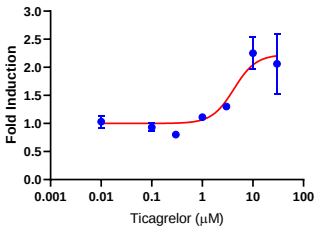	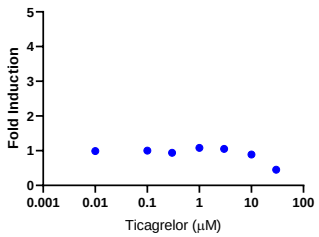	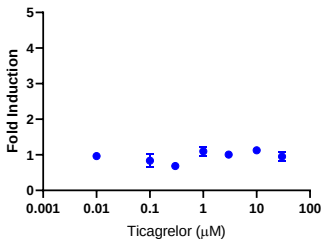
ACB (4) - 72h	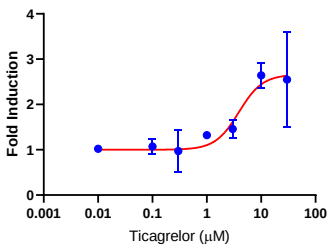	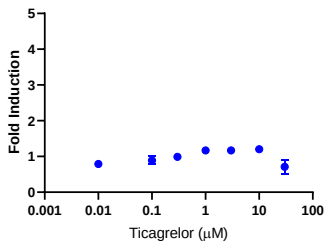	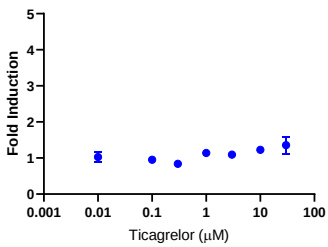

Pioglitazone	mRNA	Activity	Protein
QIE (3)	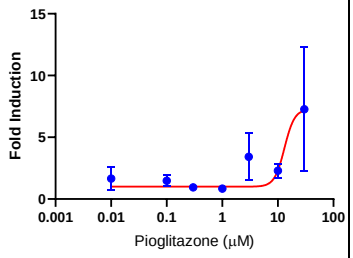	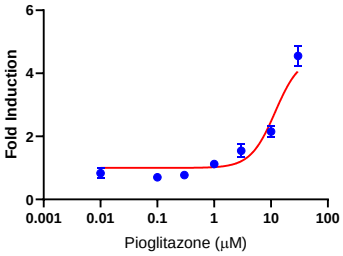	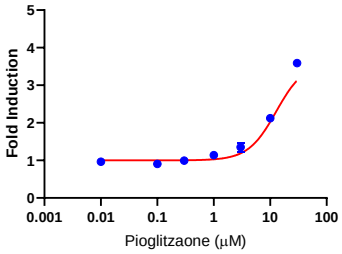
ACB (5)	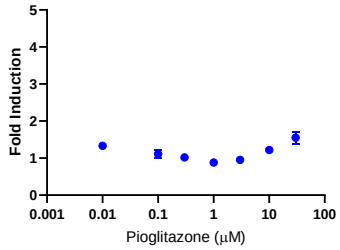	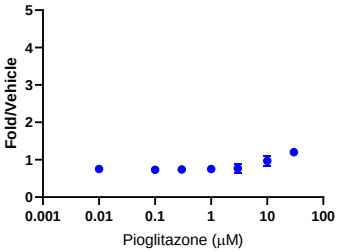	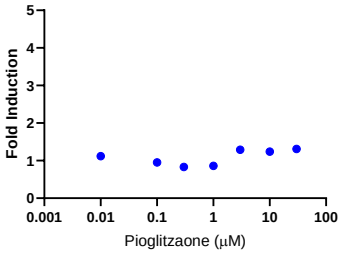
VJX (5)	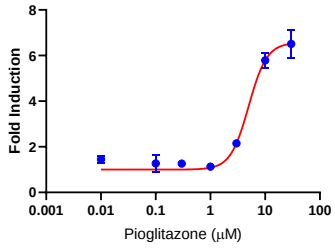	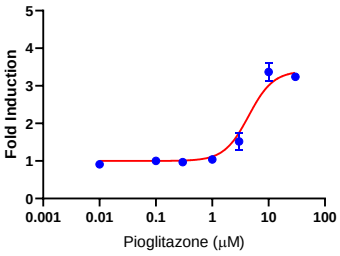	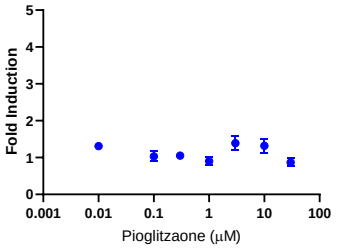

Rosiglitazone	mRNA	Activity	Protein
QIE (3)	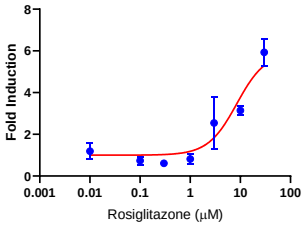	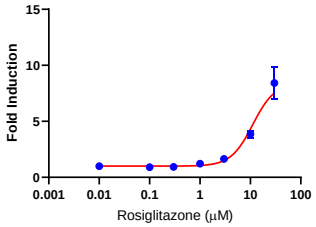	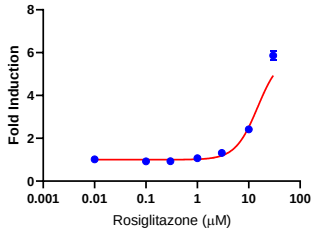
ACB (5)	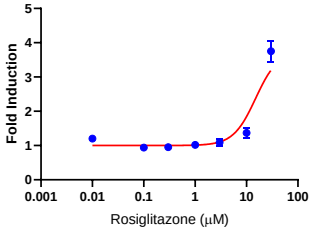	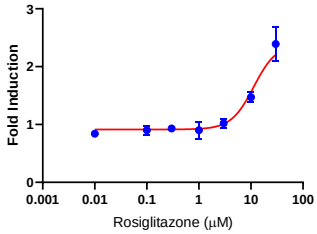	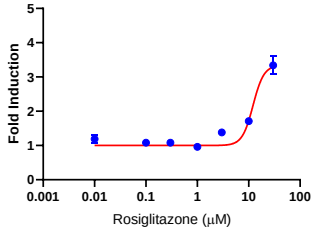
VJX (5)	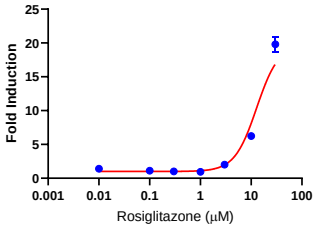	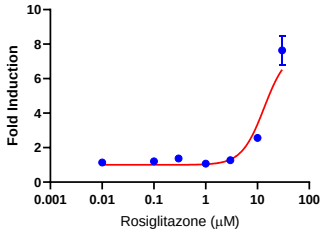	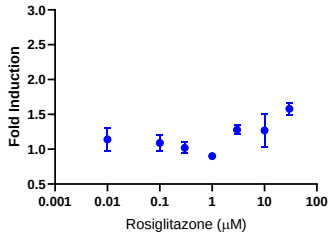

Troglitazone	mRNA	Activity	Protein
QIE (3)	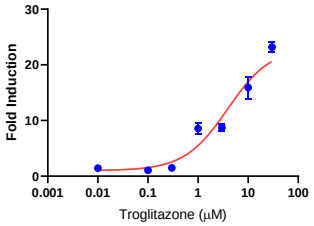	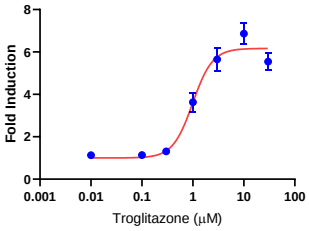	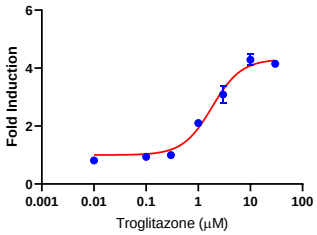
ACB (5)	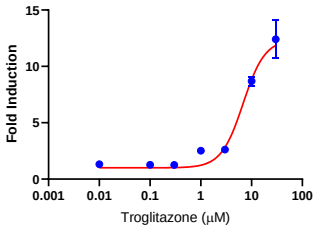	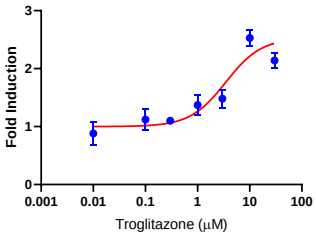	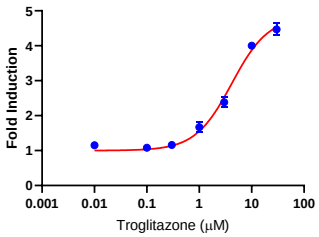
VJX (5)	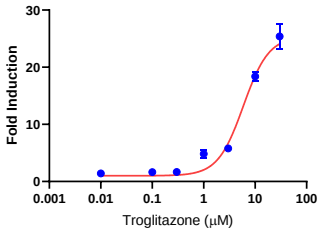	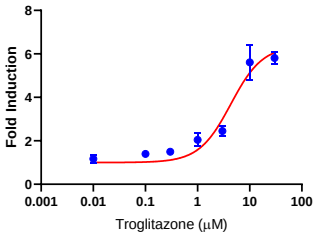	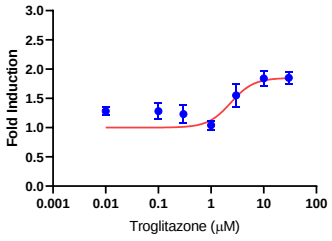

Carbamazepine	mRNA	Activity	Protein
ACB (1)	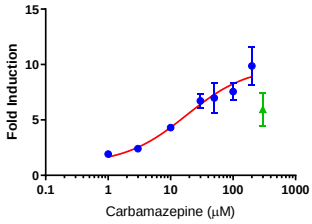	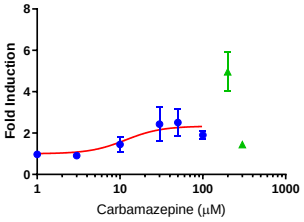	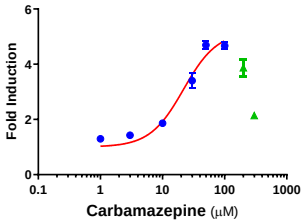
VJX (2)	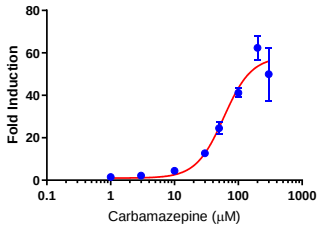	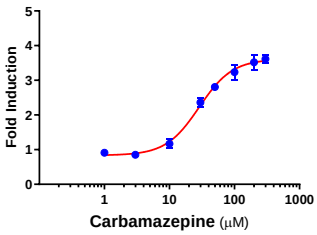	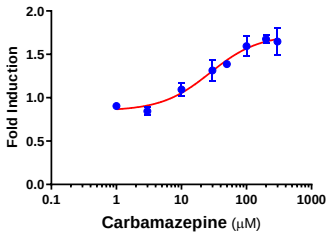

Efavirenz	mRNA	Activity	Protein
ACB (1)	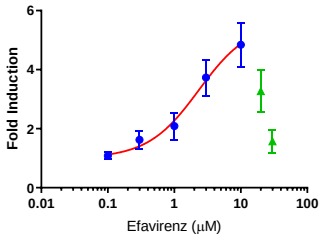	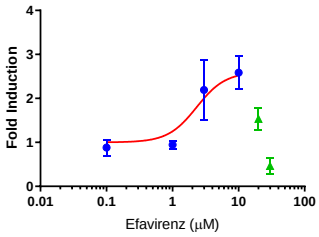	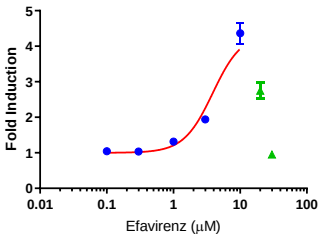
VJX (2)	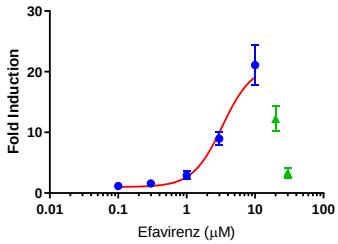	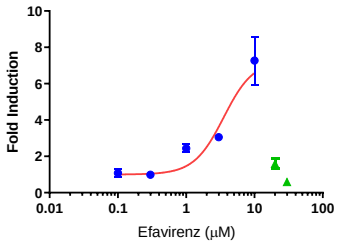	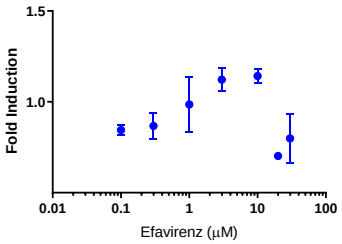

Nitrendipine	mRNA	Activity	Protein
ACB (1)	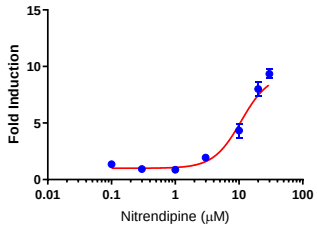	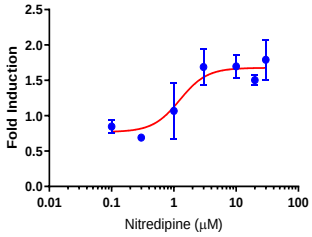	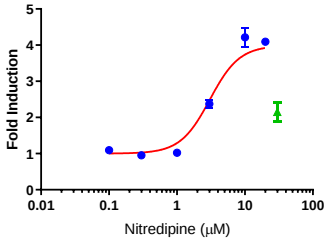
VJX (2)	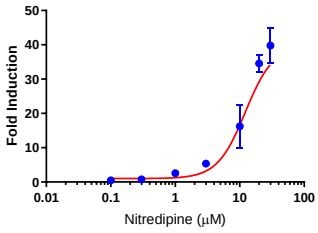	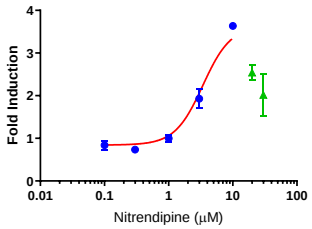	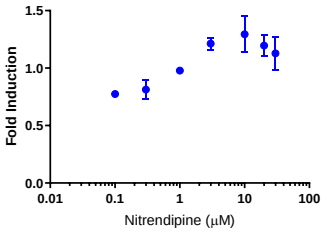

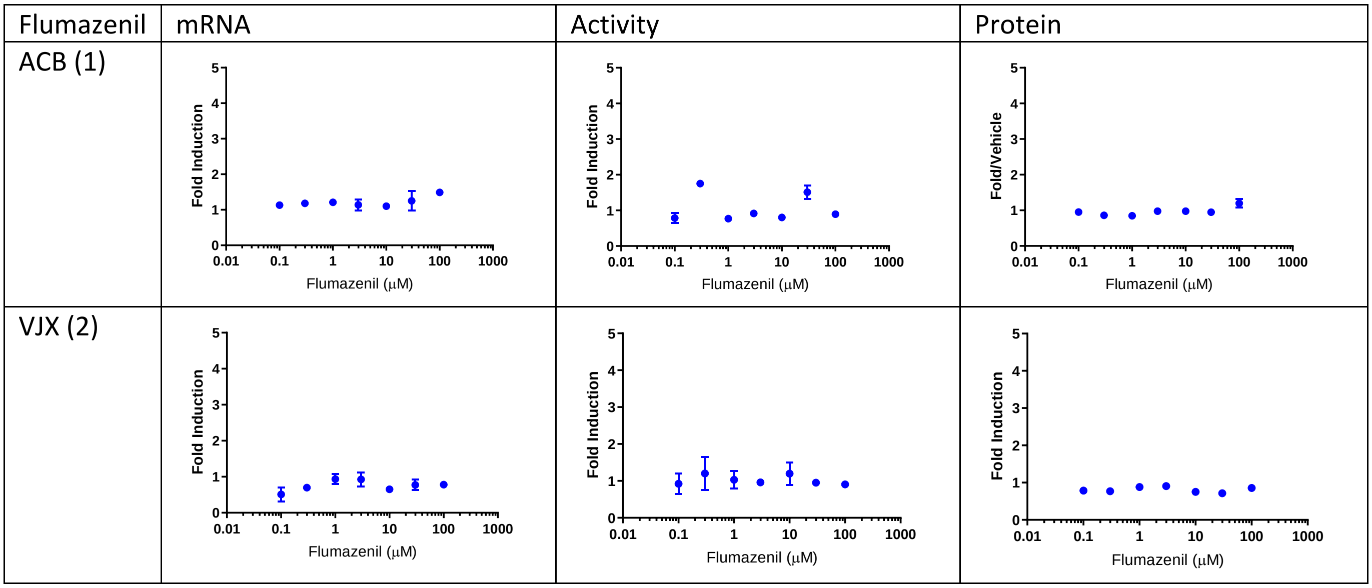

Supplemental Figure 1. Concentration-response curves for the 132 compound/donor hepatocyte experiments in this study. Blue circles represent values used in curve fitting. Green triangles represent data point excluded from curve fitting analysis, usually because values were > 20% lower than the maximum response and were at concentrations exceeding that giving the maximum response; ticagrelor at 100 μM showed evidence of cytotoxicity. Red lines represent the 4-parameter logistical fit, generated as outlined in the materials and methods. Compound data are provided as one compound per page, except rifampin which continued onto a second page. The column headers represent the quantitation endpoint used to generate the data, where mRNA, activity and protein represent data generated from RT-PCR, midazolam 1'-hydroxylase activity or LC-MS quantitation of CYP3A4 protein, according to the procedures in the methods section. Hepatocyte donor designations are shown in the far-left column. All treatment periods are for 48h, unless otherwise shown. The value in parentheses adjacent to the donor represents the experiment number. The five experiments were conducted independently over the course of 13 months.

Supplemental Figure 2. Concentration response of CYP3A4 protein induction in Donor VJX and effect of various surrogate peptides.

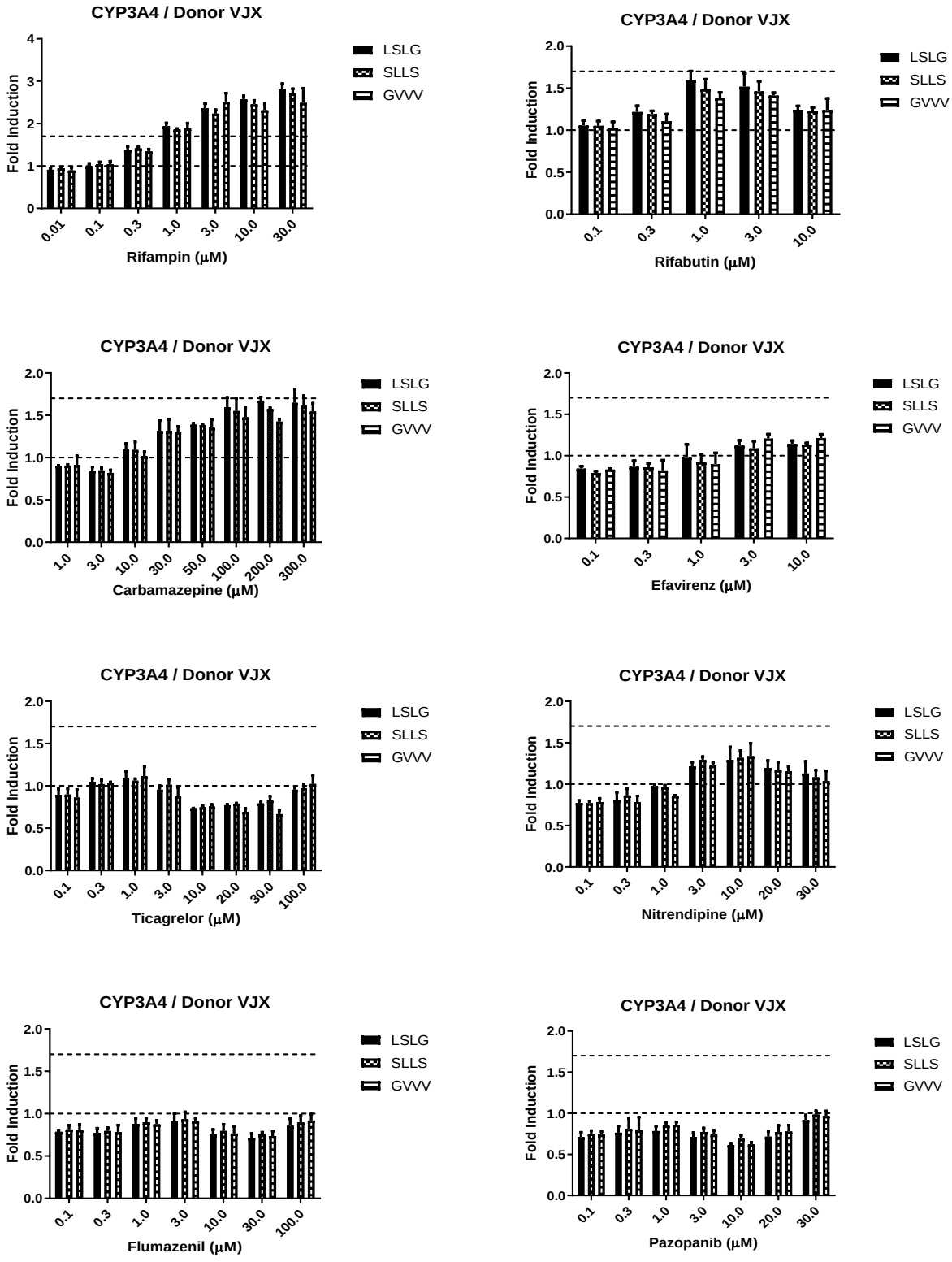

Supplemental Figure 2. Concentration response of CYP3A4 protein induction in Donor VJX and effect of various surrogate peptides. Human hepatocytes from a single donor (Donor VJX) were cultured in 96-well plates and incubated with increasing concentrations of various. LC-MS peak areas were integrated for three CYP3A4 surrogate peptides and compared to the corresponding peak areas in vehicle treated control cells. The data are presented as the fold induction compared to vehicle treated cells for each of the three peptides, abbreviated using the first four N-terminal amino acids as LSLG, SLLS, and GVVV. Data are the mean and standard deviation of triplicate wells. Levels in vehicle control wells (one-fold) and 1.7-fold induction are indicated by dashed lines.

Supplemental Figure 3. Well-to-well variability in CYP3A4 protein endpoint assay is insignificant. LC-MS peak areas for the LSLG surrogate peptide of CYP3A4 were obtained for a control plate of 96-well plated human hepatocytes. Peak areas were integrated for each well and compared to positional matched wells where vehicle treated cells typically are located in our induction assay layout. The data are presented as fold-change compared to vehicle treated positional matched wells, and presented according to their row location in the plate.

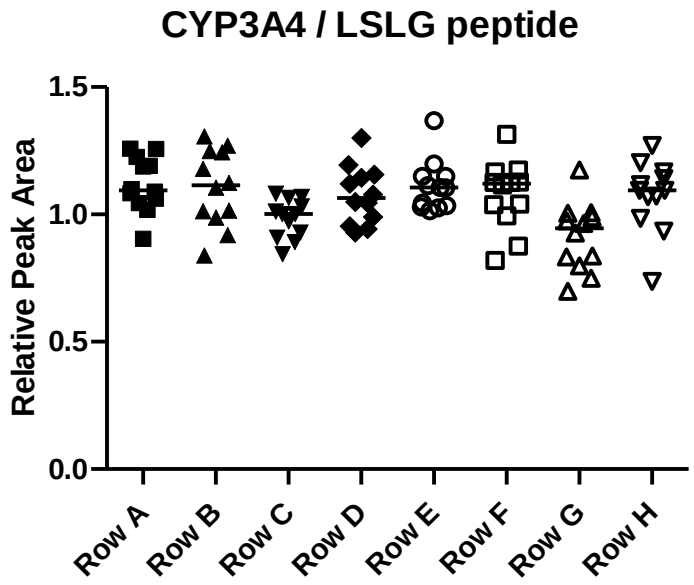

Supplemental Figure 4. Correlation analyses of the 4 compounds shown. Correlation coefficients are shown within red, white and blue squares, along with corresponding p-values in the tables to the right. Statistical significance at $p < 0.01$ is indicated by the bold and italicized numbers.

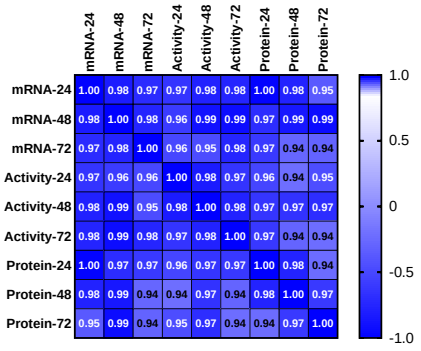

Rifampin

	mRNA-48	mRNA-72	Activity-24	Activity-48	Activity-72	Protein-24	Protein-48	Protein-72
mRNA-24	***0.0001***	***0.0000***	***0.0001***	***0.0000***	***0.0000***	***0.0000***	***0.0000***	***0.0004***
mRNA-48		***0.0001***	***0.0004***	***0.0000***	***0.0000***	***0.0002***	***0.0000***	***0.0000***
mRNA-72			***0.0002***	***0.0002***	***0.0000***	***0.0001***	***0.0005***	***0.0005***
Activity-24				***0.0000***	***0.0001***	***0.0002***	***0.0006***	***0.0002***
Activity-48					***0.0000***	***0.0001***	***0.0001***	***0.0000***
Activity-72						***0.0001***	***0.0005***	***0.0006***
Protein-24							***0.0000***	***0.0006***
Protein-48								***0.0001***

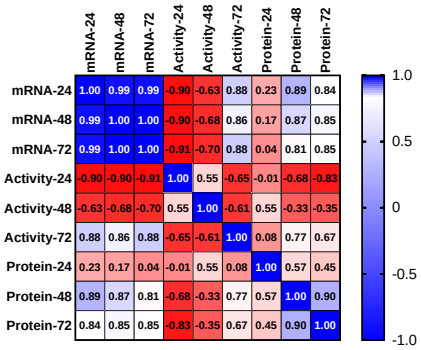

Pazopanib

	mRNA-48	mRNA-72	Activity-24	Activity-48	Activity-72	Protein-24	Protein-48	Protein-72
mRNA-24	***0.0000***	***0.0000***	***0.0064***	0.1286	***0.0092***	0.6239	***0.0067***	0.0168
mRNA-48		***0.0000***	***0.0061***	0.0902	0.0137	0.7114	0.0104	0.0143
mRNA-72			***0.0015***	0.0556	***0.0040***	0.9315	0.0144	***0.0075***
Activity-24				0.1592	0.0835	0.9834	0.0638	0.0108
Activity-48					0.1102	0.1579	0.4302	0.3984
Activity-72						0.8420	0.0268	0.0713
Protein-24							0.1375	0.2643
Protein-48								***0.0026***

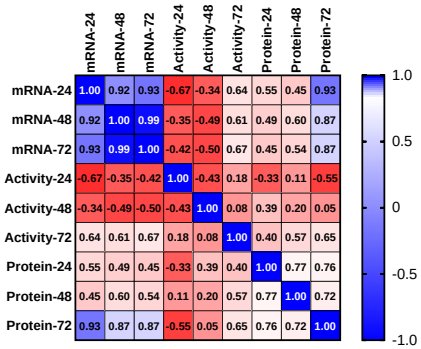

Ticagrelor

	mRNA-48	mRNA-72	Activity-24	Activity-48	Activity-72	Protein-24	Protein-48	Protein-72
mRNA-24	***0.0037***	***0.0023***	0.0984	0.5055	0.1684	0.1967	0.3053	***0.0023***
mRNA-48		***0.0000***	0.4414	0.3198	0.1996	0.2660	0.1574	***0.0100***
mRNA-72			0.3482	0.3137	0.1444	0.3079	0.2075	***0.0100***
Activity-24				0.3941	0.7332	0.4632	0.8160	0.1976
Activity-48					0.8859	0.4484	0.7102	0.9210
Activity-72						0.4309	0.2363	0.1636
Protein-24							0.0421	0.0475
Protein-48								0.0676

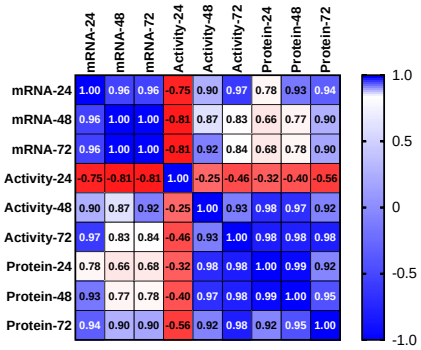

Rifabutin

	mRNA-48	mRNA-72	Activity-24	Activity-48	Activity-72	Protein-24	Protein-48	Protein-72
mRNA-24	**0.0006**	**0.0006**	0.0510	0.0392	***0.0018***	0.0390	***0.0073***	***0.0014***
mRNA-48		**0.0000**	0.0284	0.0564	0.0393	0.1037	0.0740	***0.0063***
mRNA-72			0.0269	0.0245	0.0362	0.0925	0.0652	***0.0055***
Activity-24				0.6878	0.3628	0.4815	0.4322	0.1865
Activity-48					0.0239	***0.0047***	***0.0055***	0.0251
Activity-72						***0.0004***	***0.0005***	***0.0005***
Protein-24							***0.0000***	***0.0032***
Protein-48								***0.0034***

Supplemental Table 1. Parameters used for R3 calculation

Drugs	Total Cmax (μM)	fu (plasma)	Free Cmax (μM)	Ref for Total Cmax	Ref for Fu plasma
Rifampin	10	0.12	1.2	(Fahmi et al., 2012)	(Alghamdi et al., 2018)
Pazopanib	143	0.01	1.43	(Goh et al., 2010)	(Toh et al., 2020)
Ticagrelor	7	0.01	0.07	(Dobesh and Oestreich, 2014)	(Sillen et al., 2011)
Pioglitazone	2.8	0.01	0.028	(Fahmi et al., 2012)	(Kenny et al., 2018)
Rosiglitazone	1.4	0.01	0.014	(Fahmi et al., 2012)	(Kenny et al., 2018)
Troglitazone	6.3	0.01	0.063	(Fahmi et al., 2012)	(Kenny et al., 2018)
Rifabutin	0.37	0.29	0.1073	(Fahmi et al., 2012)	(Hardman, 2001)
Carbamazepine	23	0.26	5.98	(Fahmi et al., 2012)	(Hardman, 2001)
Efavirenz	7.7	0.01	0.077	(Fahmi et al., 2012)	(Kenny et al., 2018)
Nitrendipine	0.040	0.02	0.00080	(Fahmi et al., 2012)	(Hardman, 1996)

References (Supplemental Material)

Alghamdi WA, Al-Shaer MH, and Peloquin CA (2018) Protein Binding of First-Line Antituberculosis Drugs. *Antimicrob Agents Chemother* **62**.

Dobesh PP and Oestreich JH (2014) Ticagrelor: pharmacokinetics, pharmacodynamics, clinical efficacy, and safety. *Pharmacotherapy* **34:**1077-1090.

Fahmi OA, Raucy JL, Ponce E, Hassanali S, and Lasker JM (2012) Utility of DPX2 cells for predicting CYP3A induction-mediated drug-drug interactions and associated structure-activity relationships. *Drug Metab Dispos* **40:**2204-2211.

Goh BC, Reddy NJ, Dandamudi UB, Laubscher KH, Peckham T, Hodge JP, Suttle AB, Arumugham T, Xu Y, Xu CF, Lager J, Dar MM, and Lewis LD (2010) An evaluation of the drug interaction potential of pazopanib, an oral vascular endothelial growth factor receptor tyrosine kinase inhibitor, using a modified Cooperstown 5+1 cocktail in patients with advanced solid tumors. *Clin Pharmacol Ther* **88:**652-659.

Hardman JG, Limbird, Lee E., Goodman Gilman, Alfred (2001) *Goodman & Gilman's The Pharmacological Basis of Therapeutics, 10th edition*. McGraw-Hill.

Hardman JG, Limbird, Lee E., Molinoff, Perry B., Ruddon, Raymond W., Goodman Gilman, Alfred (1996) *Goodman & Gilman's the pharmacological basis of therapeutics, 9th edition*. McGraw-Hill.

Kenny JR, Ramsden D, Buckley DB, Dallas S, Fung C, Mohutsky M, Einolf HJ, Chen L, Dekeyser JG, Fitzgerald M, Goosen TC, Siu YA, Walsky RL, Zhang G, Tweedie D, and Hariparsad N (2018) Considerations from the Innovation and Quality Induction Working Group in Response to Drug-Drug Interaction Guidances from Regulatory Agencies: Focus on CYP3A4 mRNA In Vitro Response Thresholds, Variability, and Clinical Relevance. *Drug Metab Dispos* **46:**1285-1303.

Sillen H, Cook M, and Davis P (2011) Determination of unbound ticagrelor and its active metabolite (AR-C124910XX) in human plasma by equilibrium dialysis and LC-MS/MS. *J Chromatogr B Analyt Technol Biomed Life Sci* **879:**2315-2322.

Toh YL, Pang YY, Shwe M, Kanesvaran R, Toh CK, Chan A, and Ho HK (2020) HPLC-MS/MS coupled with equilibrium dialysis method for quantification of free drug concentration of pazopanib in plasma. *Heliyon* **6:**e03813.